Electronic Supplementary Material (ESI) for Dalton Transactions.
This journal is © The Royal Society of Chemistry 2014

Electronic Supplementary Information

Versatile Redox Reactivity of triaryl-*meso*-substituted Ni(II) Porphyrin

Abdou K. D. Dimé, Charles H. Devillers,* Hélène Cattey and Dominique Lucas*
Institut de Chimie Moléculaire de l'Université de Bourgogne, UMR CNRS 6302, Université de Bourgogne, BP 47870, 21078 DIJON Cedex, France.
E-mail: charles.devillers@u-bourgogne.fr; dominique.lucas@u-bourgogne.fr

Contents

Characterisation of **1-Ni**, **1-Ni-Cl** and **1-Ni-P**$^+$:

-*Characterisation of **1-Ni***:

^{1}H NMR (**Fig. 1** and **Fig. 2**) S3-4
^{13}C NMR (**Fig. 3** and **Fig. 4**) S5-6
COSY NMR (**Fig. 5** and **Fig. 6**) S7-8
NOESY NMR (**Fig. 7** and **Fig. 8**) S9-10
HSQC NMR (**Fig. 9** and **Fig. 10**) S11-12

-*Characterisation of **1-Ni-Cl***:

^{1}H NMR (**Fig. 11** and **Fig. 12**) S13-14
^{13}C NMR (**Fig. 13** and **Fig. 14**) S15-16
COSY NMR (**Fig. 15** and **Fig. 16**) S17-18
NOESY NMR (**Fig. 17** and **Fig. 18**) S19-20
HSQC NMR (**Fig. 19** and **Fig. 20**) S21-22
MALDI-TOF MS of **1-Ni-Cl** (**Fig. 21**) S23

-*Characterisation of **1-Ni-P**$^+$*:

^{1}H NMR (**Fig. 22** and **Fig. 23**) S23-24
^{13}C NMR (**Fig. 24** and **Fig. 25**) S25-26
COSY NMR (**Fig. 26** and **Fig. 27**) S27-28
NOESY NMR (**Fig. 28** and **Fig. 29**) S29-30
HSQC NMR (**Fig. 30** and **Fig. 31**) S31-32

^{31}P NMR (**Fig. 32**) S33
MALDI-TOF MS of **1-Ni-P^{+}** (**Fig. 33**) S33

Electrolysis of **1-Ni** in DMF:
Maldi-Tof mass spectrum of the crude solution after electrolysis (**Fig. 34**) S34
RDE voltammetry before and after electrolysis (**Fig. 35**) S34
UV-Vis absorption spectrum of the diluted crude solution (in CH_2Cl_2) resulting from electrolysis of **1-Ni** in DMF (**Fig. 36**) S35

Chemical synthesis of **3-Ni** and **2-Ni** S36
*Characterisation of **3-Ni***
MALDI-TOF mass spectrum (**Fig. 37**) S36
^{1}H NMR in $CDCl_3$ (**Fig. 38** and **Fig. 39**) S37
Characterisation of **2-Ni**
MALDI-TOF mass spectrum (**Fig. 40**) S39
^{1}H NMR in CD_2Cl_2 (**Fig. 41** and **Fig. 42**) S41

Chemical synthesis of **2'-Ni** S42
*Characterisation of **2'-Ni***
Full (top) and partial (bottom) ^{1}H NMR spectra of **2'Ni** (**Fig. 43**) S42
UV-vis. absorption spectrum of **2'-Ni** in CH_2Cl_2 (**Fig. 44**) S43
MALDI-TOF mass spectrum of **2'-Ni** (**Fig. 45**) S44

Example of calculation of product's distribution from the ^{1}H NMR spectrum of the crude obtained in the conditions of entry 2, Table 1 of the manuscript (CD_2Cl_2, 300 MHz, 300 K) (**Fig. 46**) S44

Crystal and structure refinement data for **1-Ni**, **1-Ni-Cl**, **1-Ni-P^{+}** and **3-Ni** (**Table S1**). S47

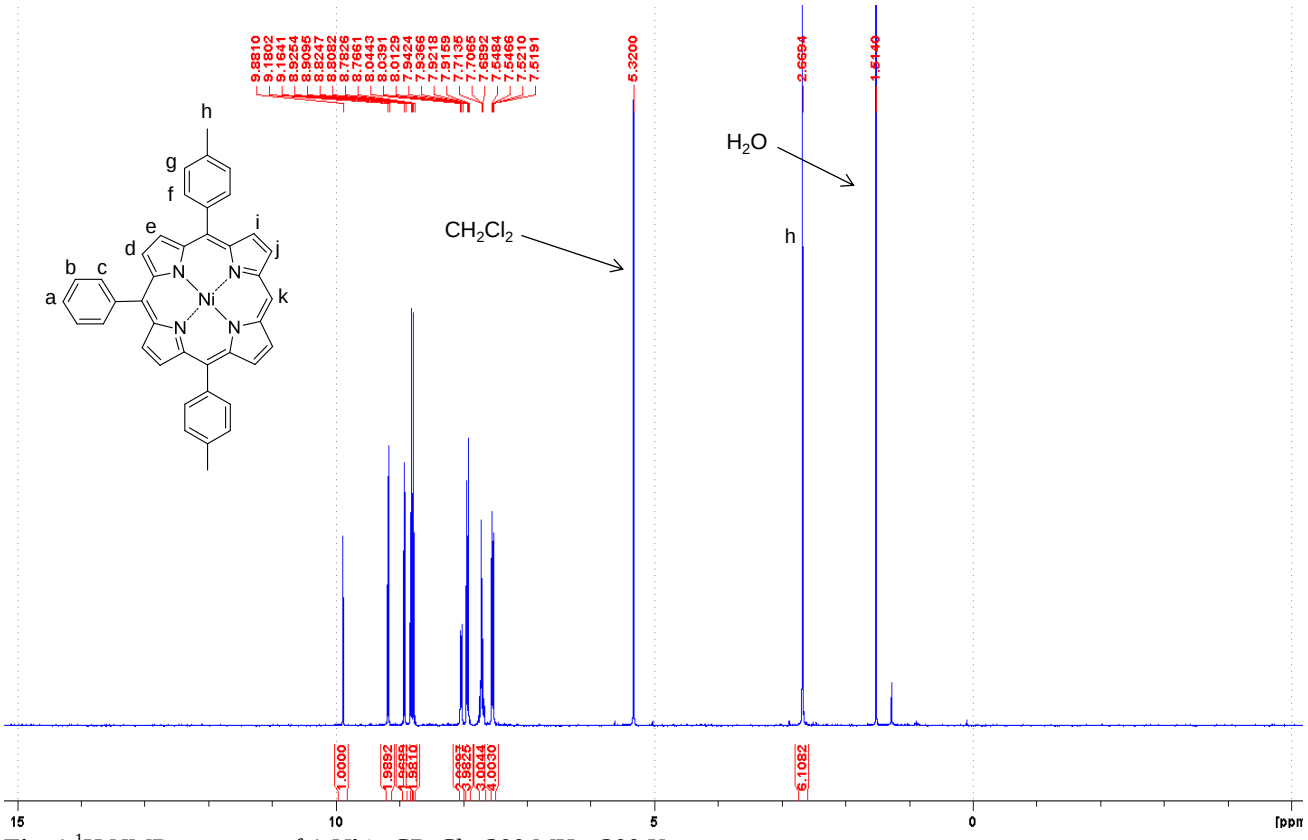

Fig. 1 ^{1}H NMR spectrum of **1-Ni** in CD_2Cl_2, 300 MHz, 300 K.

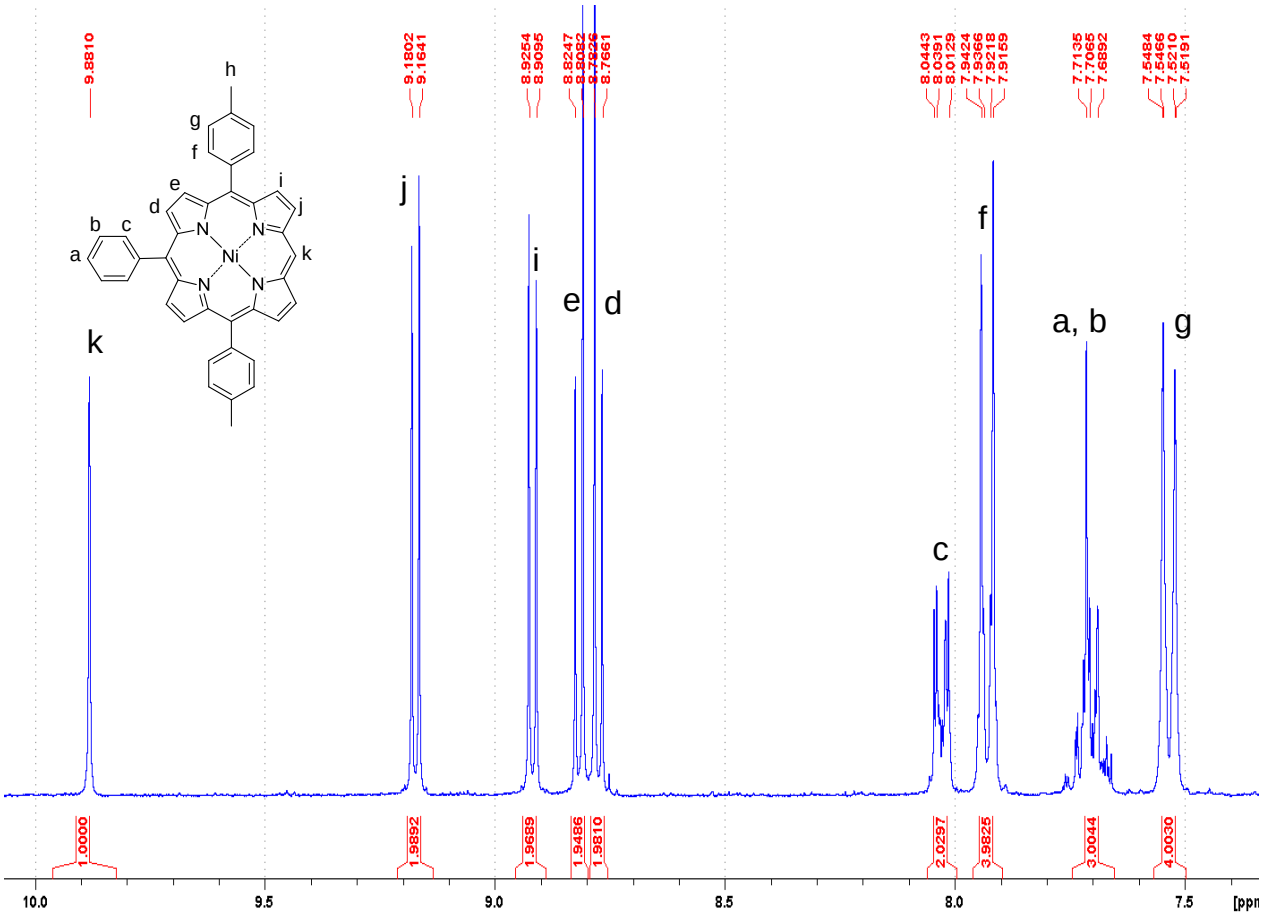

Fig. 2 Partial ^{1}H NMR spectrum of **1-Ni** in CD_2Cl_2, 300 MHz, 300 K. δ (ppm) 2.67 (s, CH_3, 6H), 7.53 (d, ^{3}J = 7.7 Hz, *m*-Tol, 4H), 7.66-7.76 (m, *m*-and *p*-Ph, 3H), 7.93 (d, ^{3}J = 7.9 Hz, *o*-Tol, 4H), 8.01-8.05 (m, *o*-Ph, 2H), 8.77 (d, ^{3}J = 4.9 Hz, β-Pyrr, 2H), 8.82 (d, ^{3}J = 4.9 Hz, β-Pyrr, 2H), 8.92 (d, ^{3}J = 4.8 Hz, β-Pyrr, 2H), 9.17 (d, ^{3}J = 4.6 Hz, β-Pyrr, 2H), 9.88 (s, β-Pyrr, 1H).

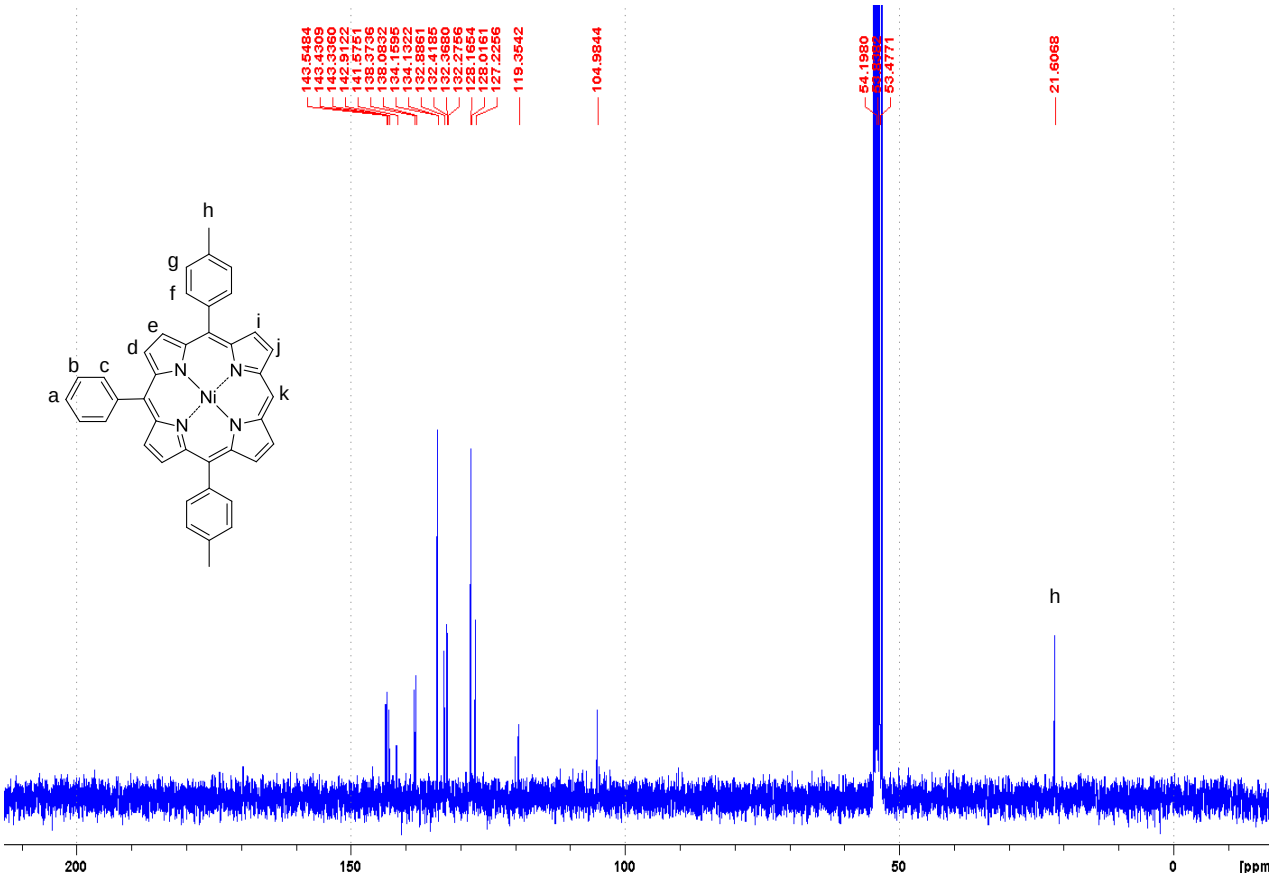

Fig. 3 ^{13}C NMR spectrum of **1-Ni** in CD_2Cl_2, 75 MHz, 300 K.

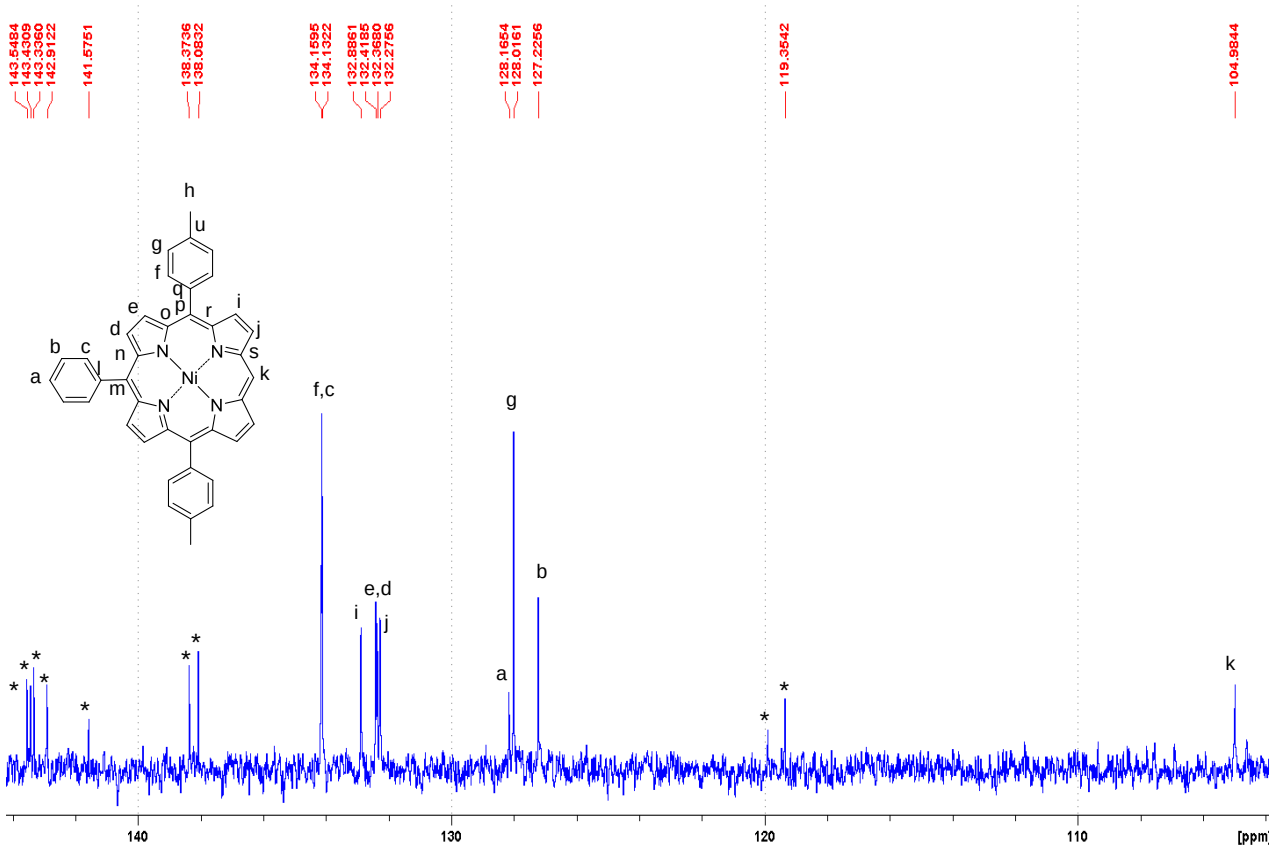

Fig. 4 Partial ^{13}C NMR spectrum of **1-Ni** in CD_2Cl_2, 75 MHz, 300 K.
(*): non attributed signals. These signals could be: l, m, n, o, p, q, u, r, and s (these 9 C are uncoupled with proton signals in the ^{1}H-^{13}C HSQC experiment).

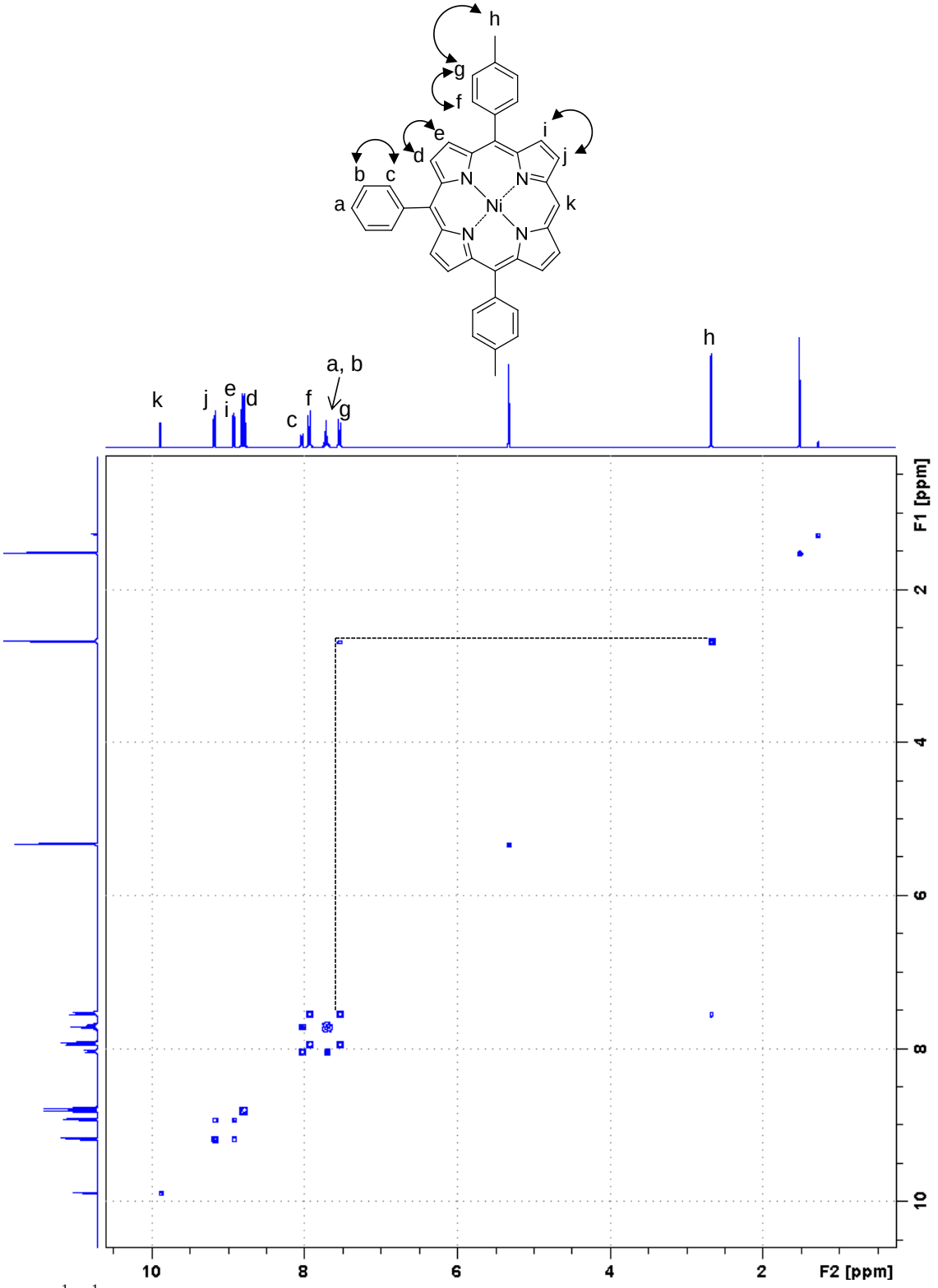

Fig. 5 ^{1}H-^{1}H COSY NMR spectrum of **1-Ni** in CD_2Cl_2, 300 MHz, 300 K.

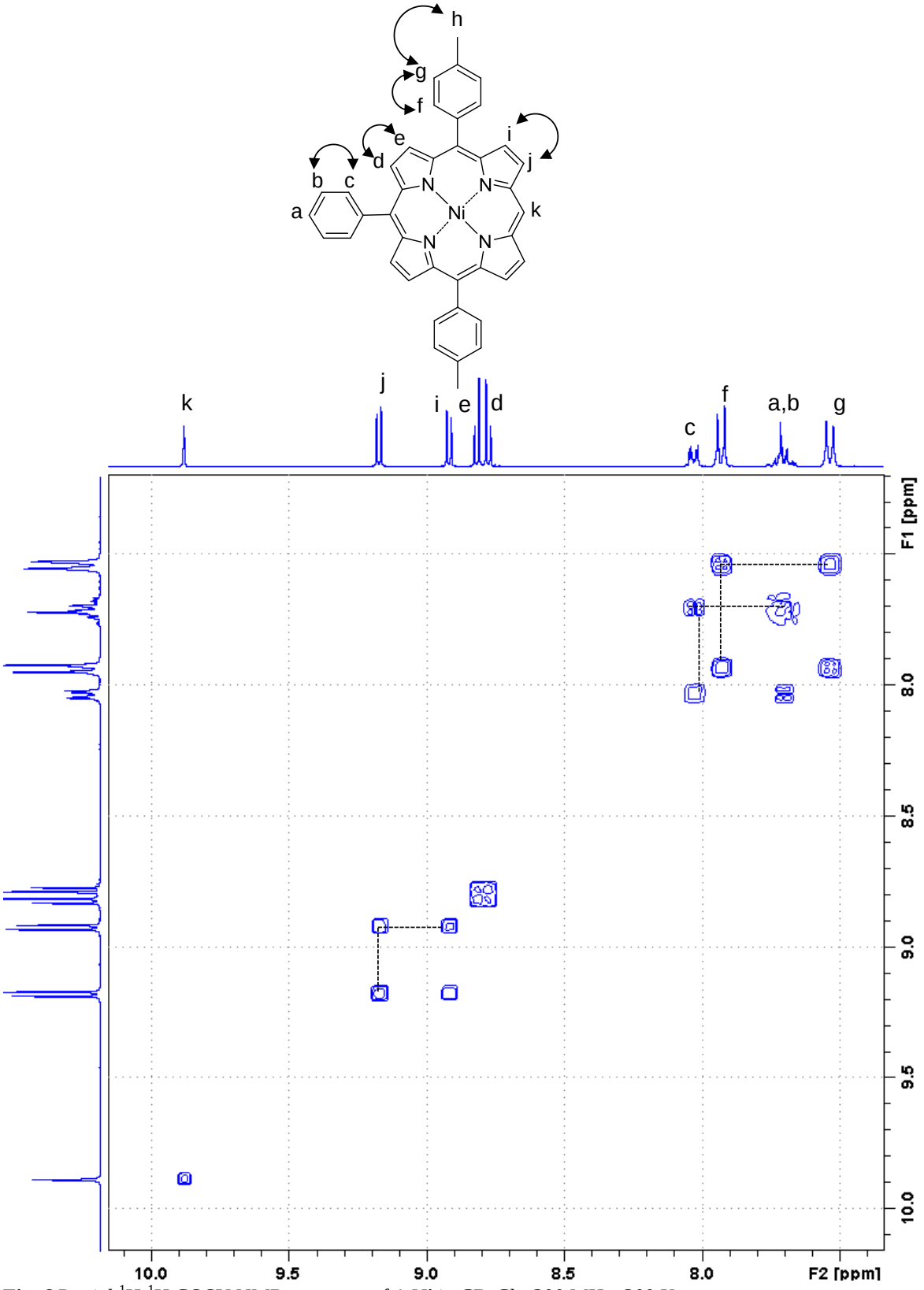

Fig. 6 Partial ^{1}H-^{1}H COSY NMR spectrum of **1-Ni** in CD_2Cl_2, 300 MHz, 300 K.

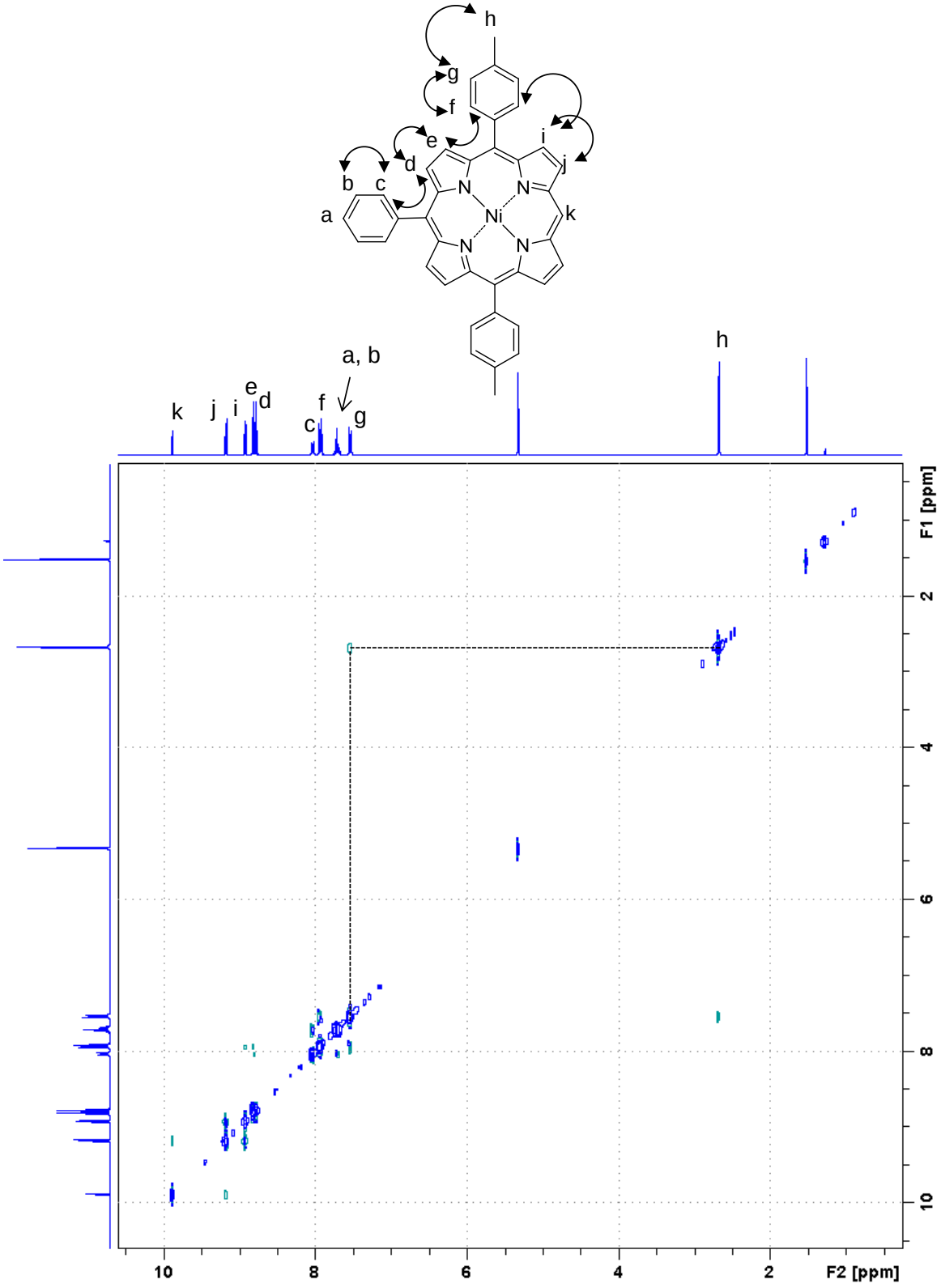

Fig. 7 ^{1}H-^{1}H NOESY NMR spectrum of **1-Ni** in CD_2Cl_2, 300 MHz, 300 K.

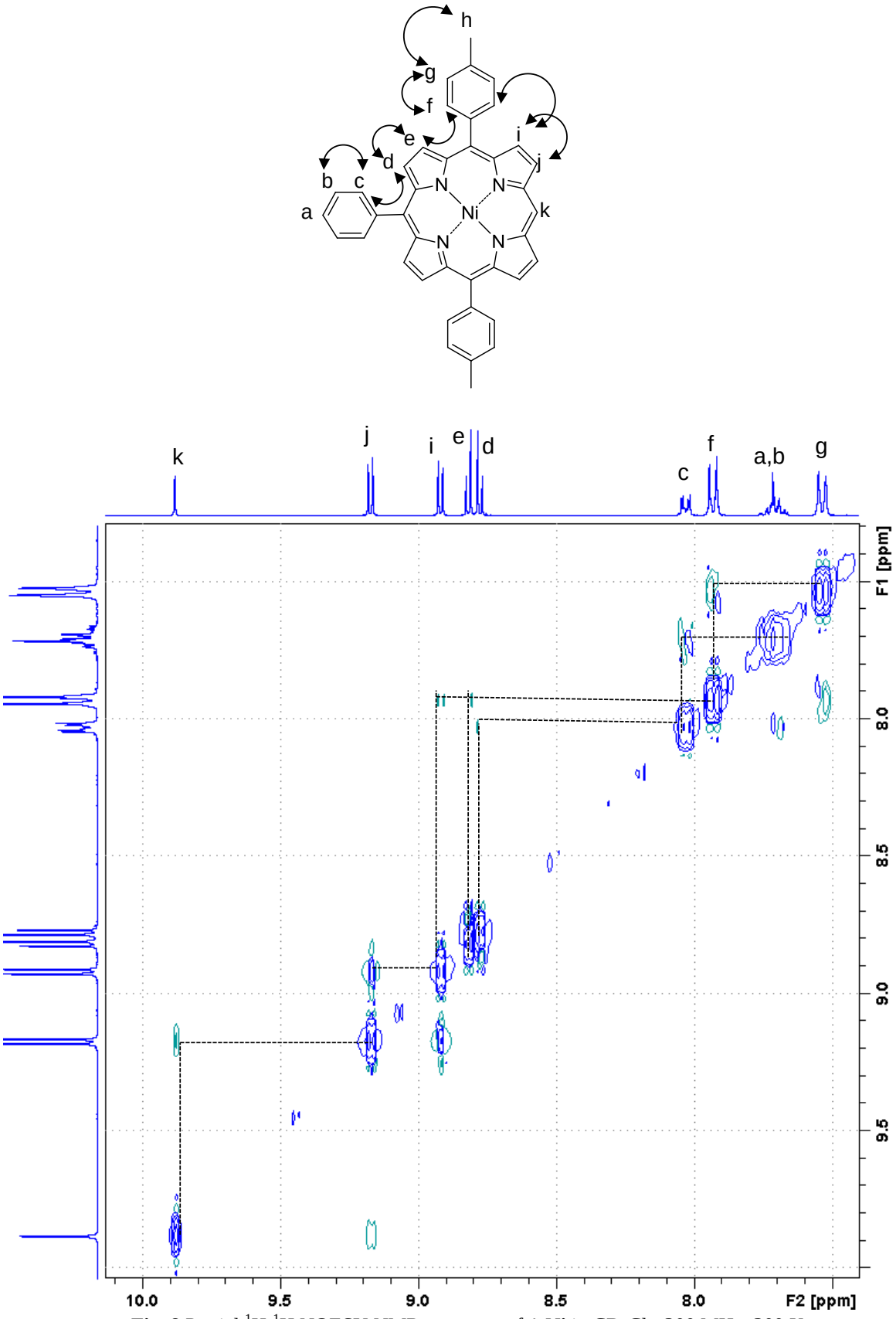

Fig. 8 Partial ^{1}H-^{1}H NOESY NMR spectrum of **1-Ni** in CD_2Cl_2, 300 MHz, 300 K.

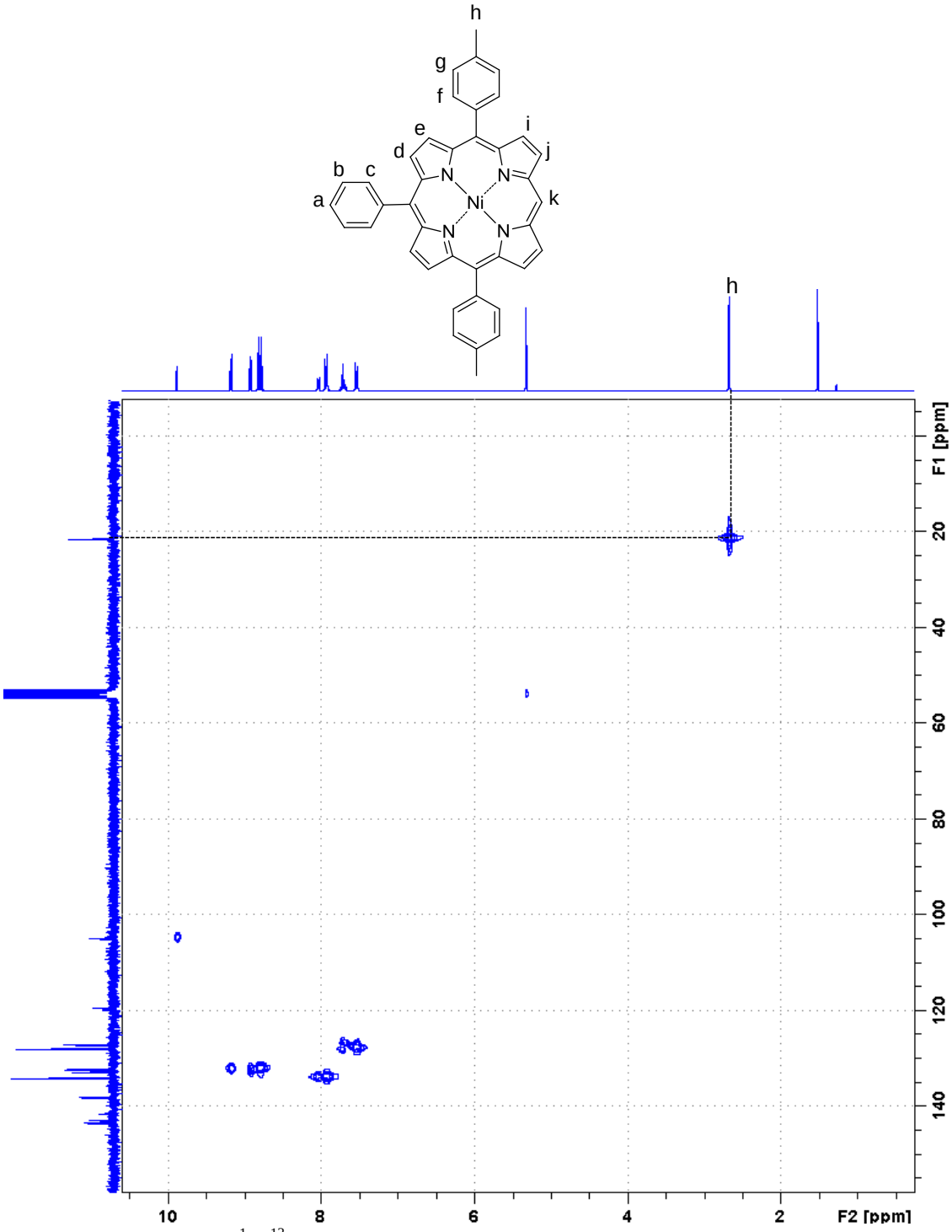

Fig. 9 ^{1}H-^{13}C HSQC NMR spectrum of **1-Ni** in CD_2Cl_2, 300 MHz, 300 K.

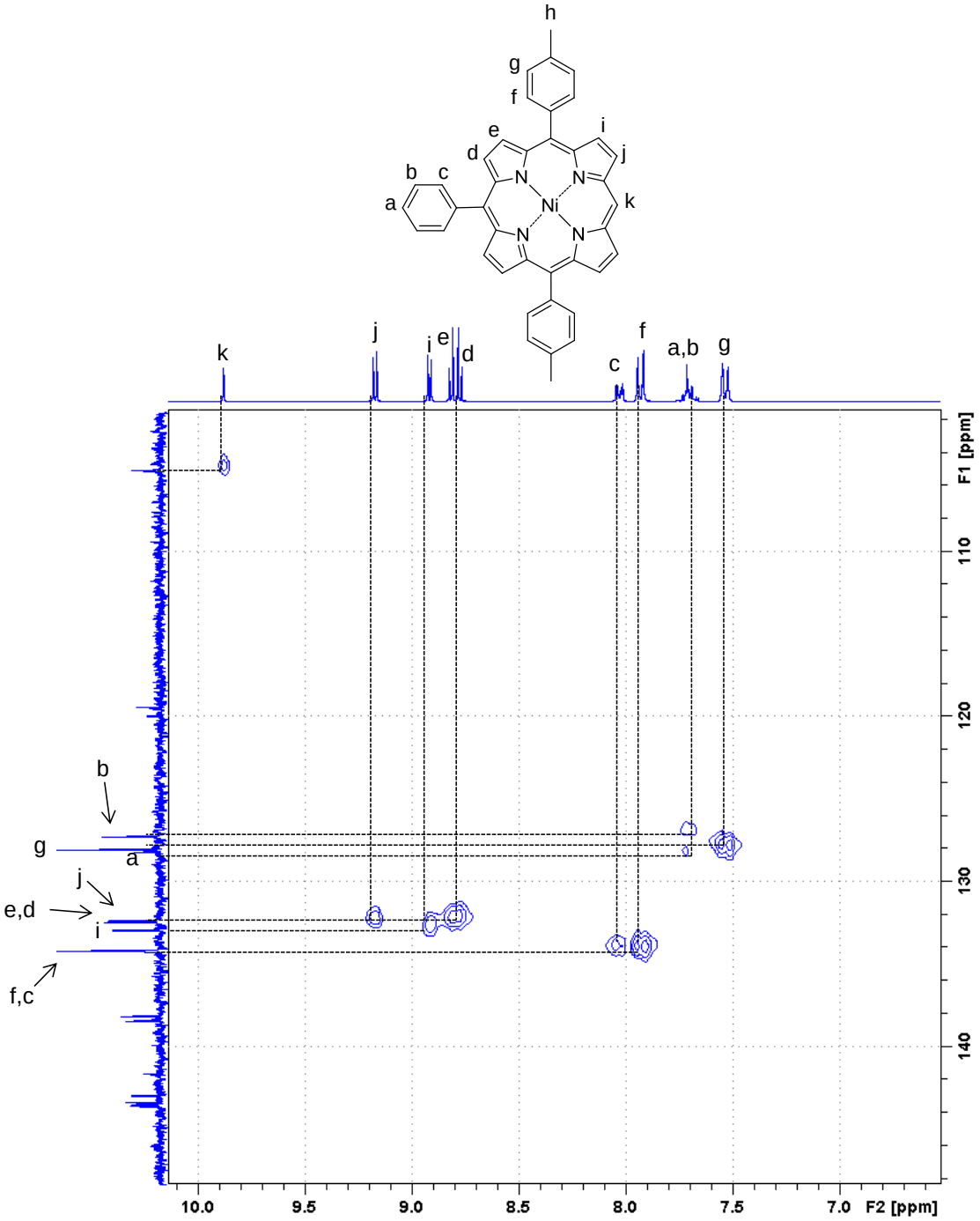

Fig. 10 Partial ^{1}H-^{13}C HSQC NMR spectrum of **1-Ni** in CD_2Cl_2, 300 MHz, 300 K.

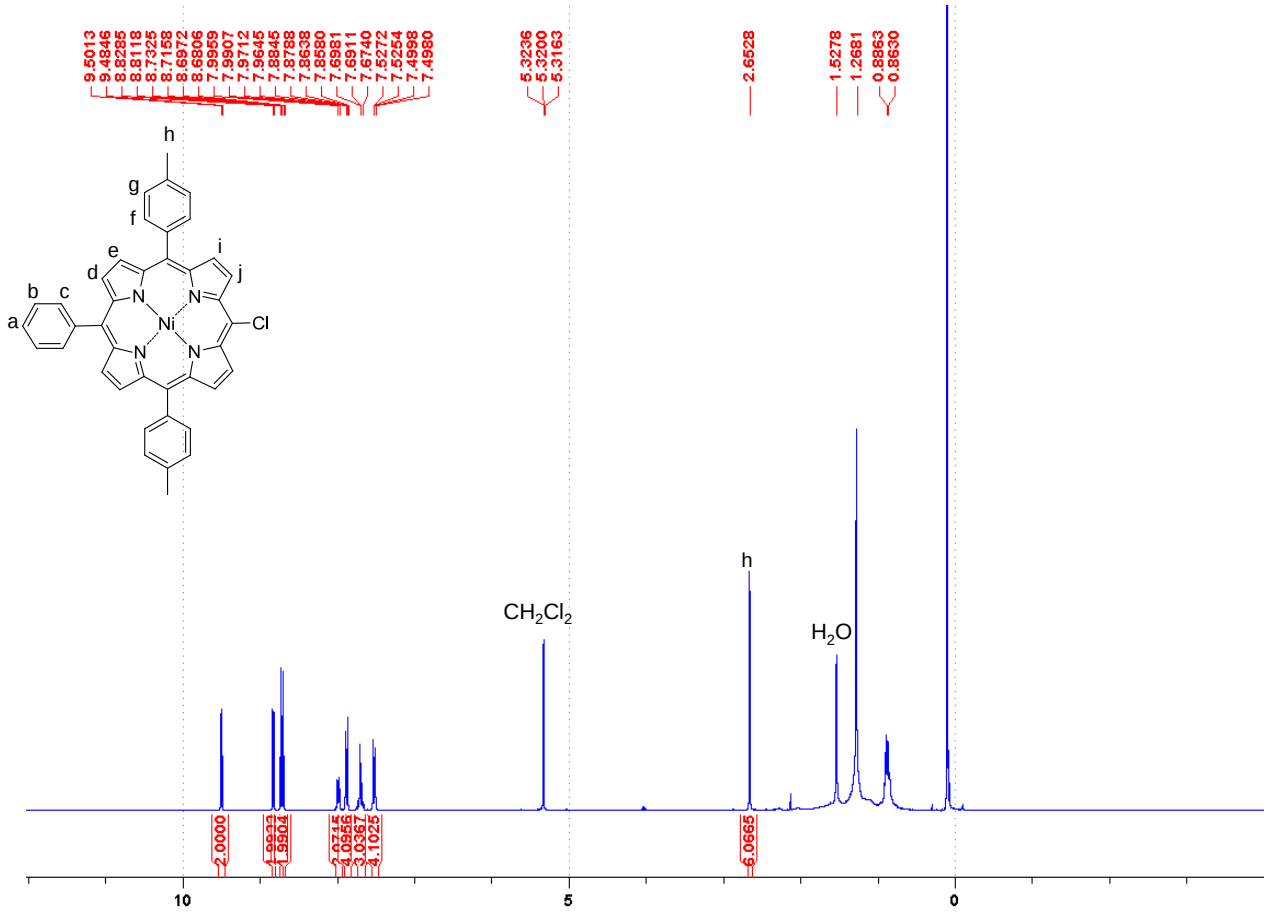

Fig. 11 ^{1}H NMR spectrum of **1-Ni-Cl** in CD_2Cl_2, 300 MHz, 300 K.

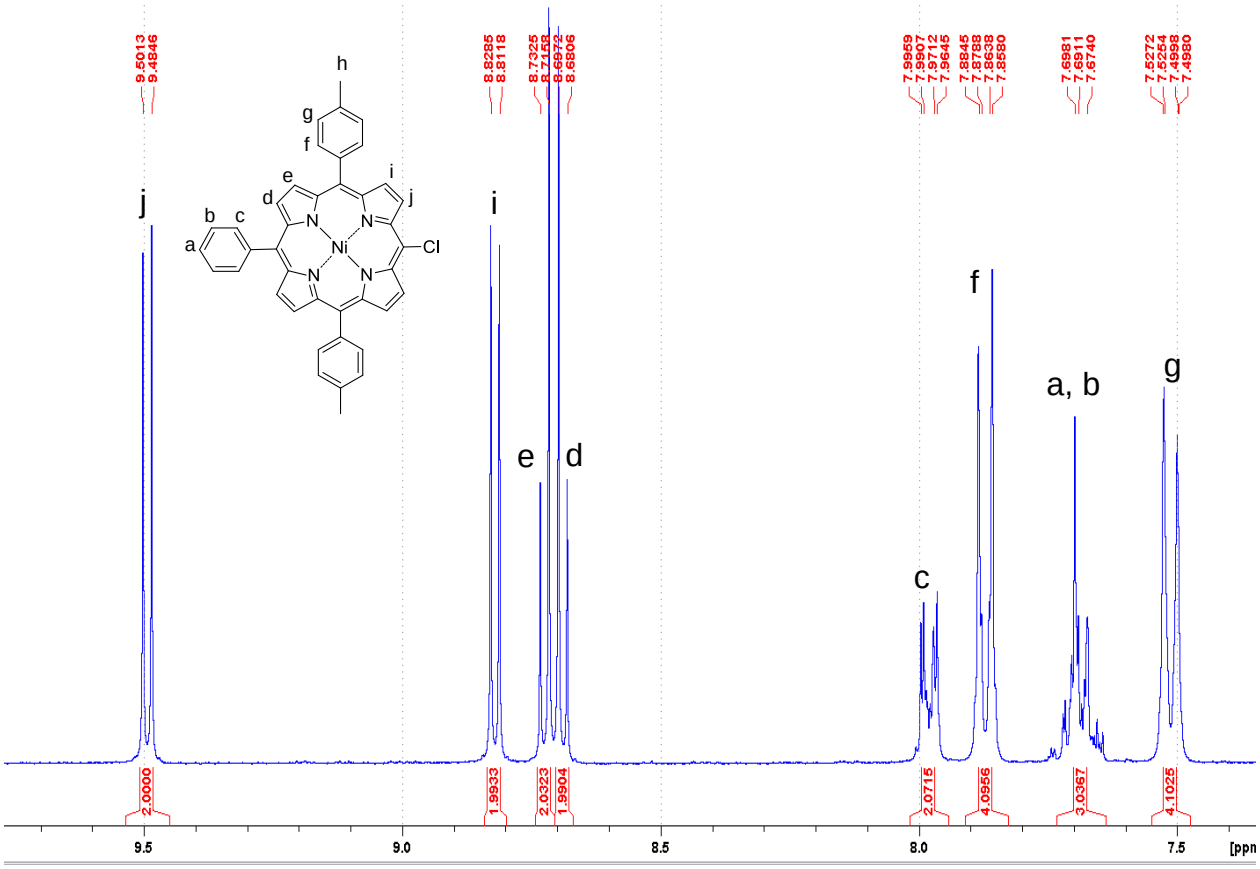

Fig. 12 Partial ^{1}H NMR spectrum of **1-Ni-Cl** in CD_2Cl_2, 300 MHz, 300 K. δ (ppm) 2.65 (s, CH_3, 6H), 7,51 (d, ^{3}J = 7.7 Hz, *m*-Tol, 4H), 7.64-7.74 (m, *m*-and *p*-Ph, 3H), 7,87 (d, ^{3}J = 7.7 Hz, *o*-Tol, 4H), 7.96-8.00 (m, *o*-Ph, 2H), 8,69 (d, ^{3}J = 5.0 Hz, β-Pyrr, 2H), 8.72 (d, ^{3}J = 5.0 Hz, β-Pyrr, 2H), 8.82 (d, ^{3}J = 5.0 Hz, β-Pyrr, 2H), 9.49 (d, ^{3}J = 5.0 Hz, β-Pyrr, 2H).

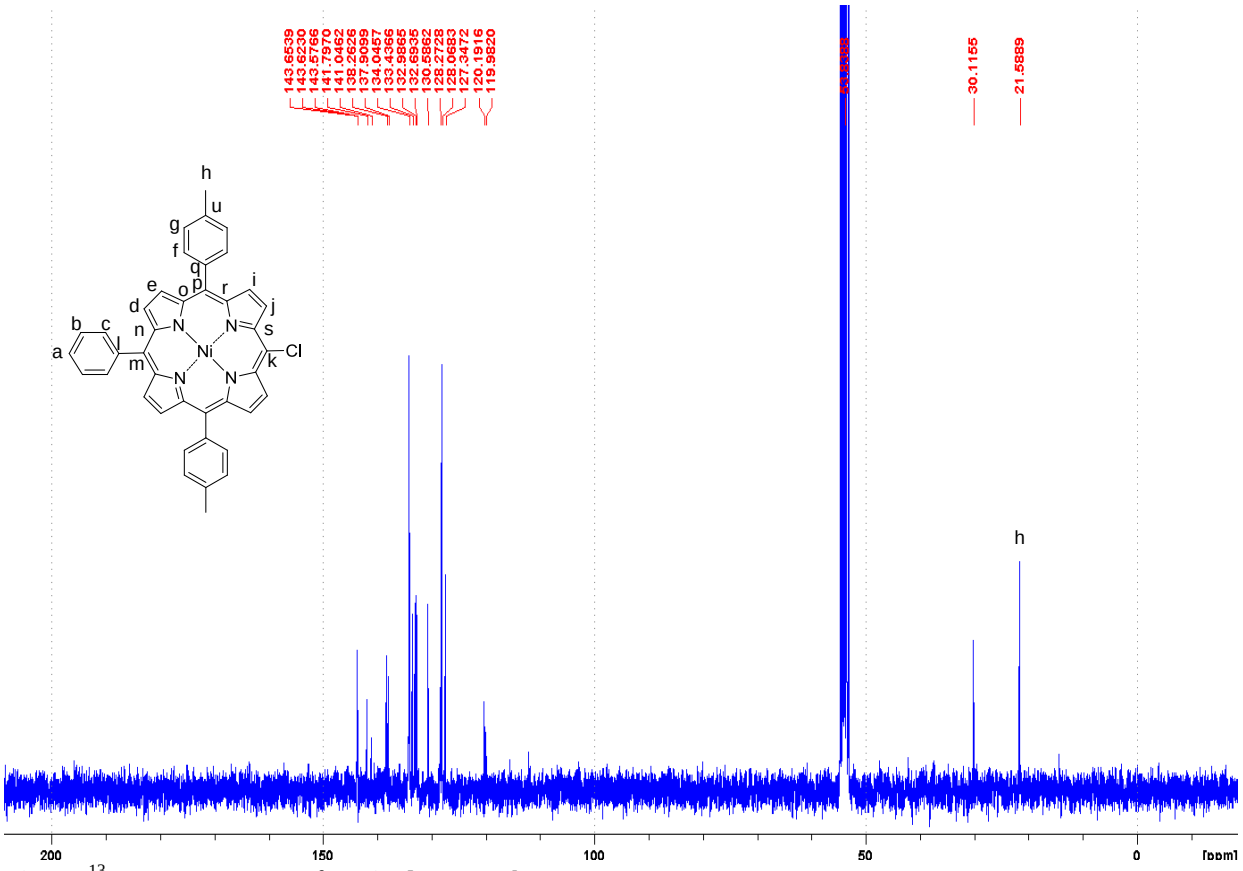

Fig. 13 ^{13}C NMR spectrum of **1-Ni-Cl** in CD_2Cl_2, 75 MHz, 300 K.

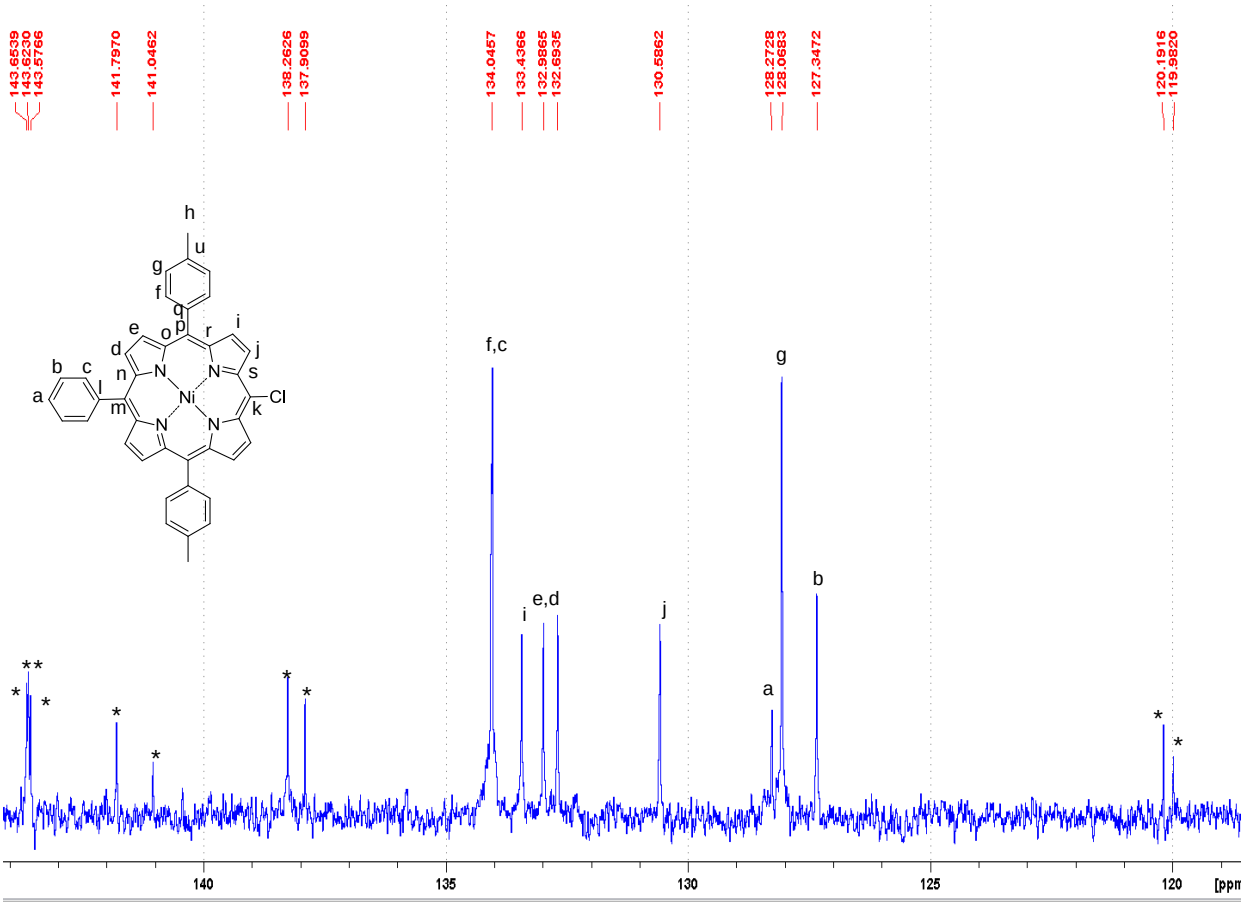

Fig. 14 Partial ^{13}C NMR spectrum of **1-Ni-Cl** in CD_2Cl_2, 75 MHz, 300 K. (*): non attributed signals. These signals could be: l, m, n, o, p, q, u, r, and s (these 9 C are uncoupled with proton signals in the ^{1}H-^{13}C HSQC experiment).

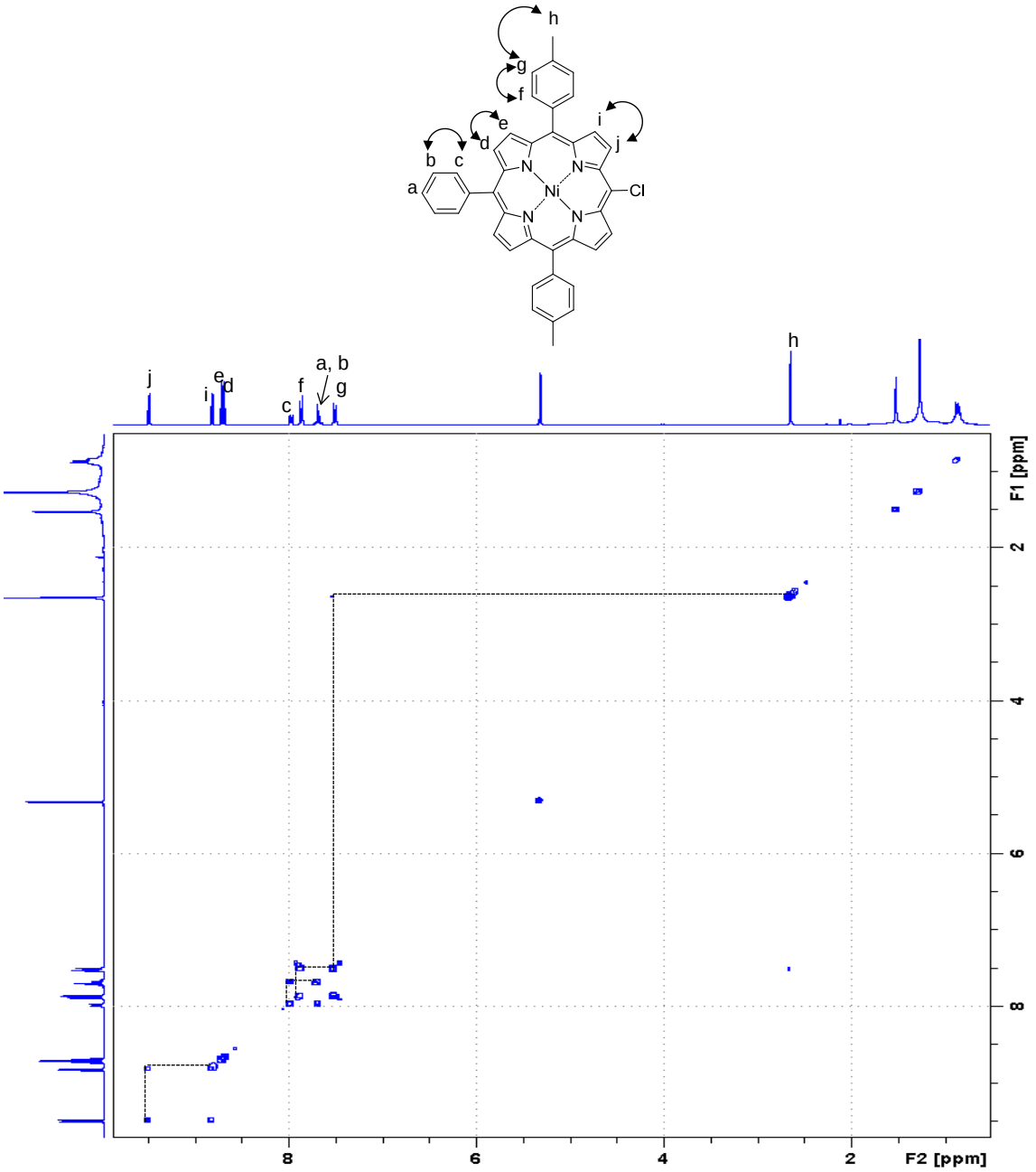

Fig. 15 ^{1}H-^{1}H COSY NMR spectrum of **1-Ni-Cl** in CD_2Cl_2, 300 MHz, 300 K.

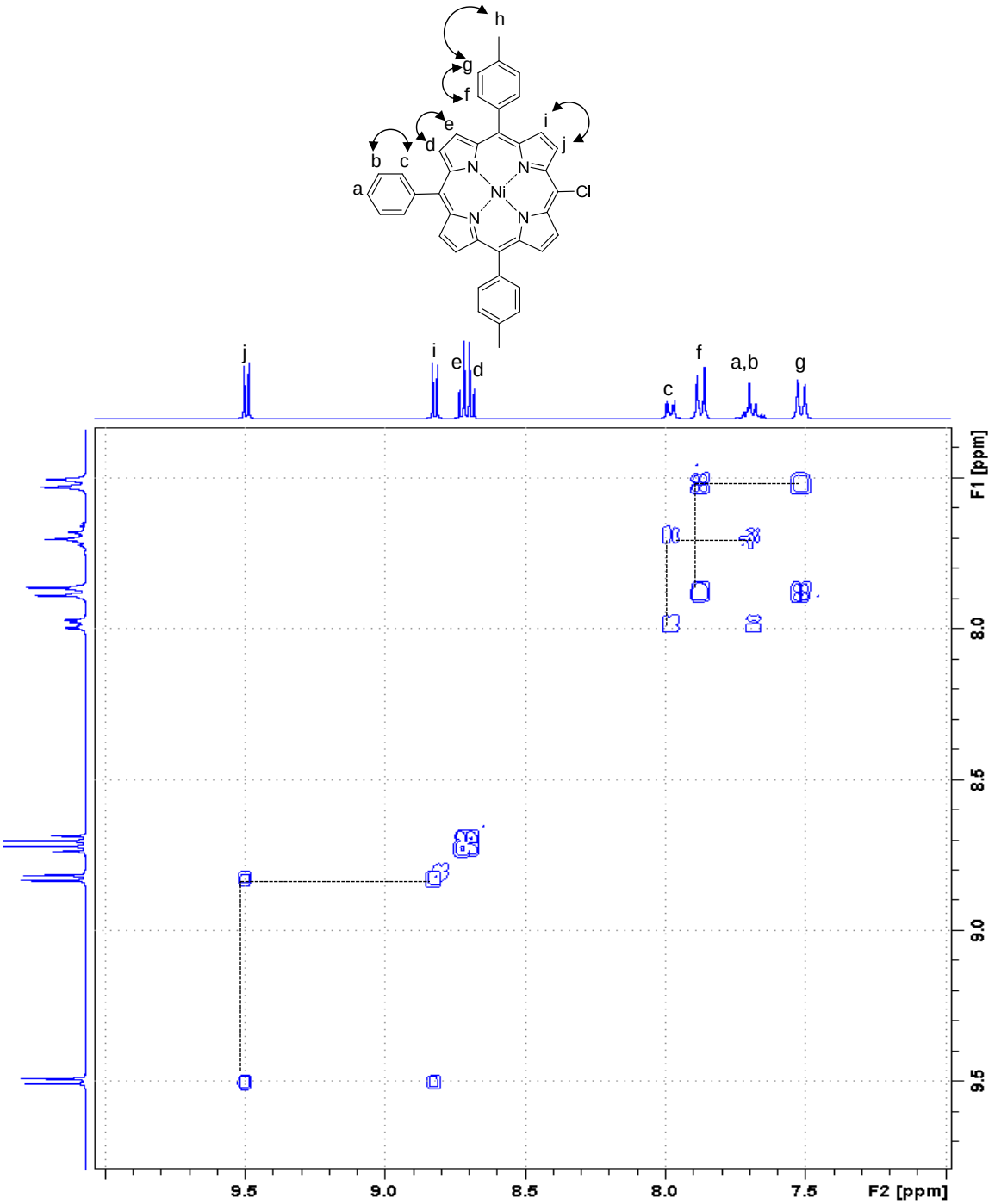

Fig. 16 Partial ^{1}H-^{1}H COSY NMR spectrum of **1-Ni-Cl** in CD_2Cl_2, 300 MHz, 300 K.

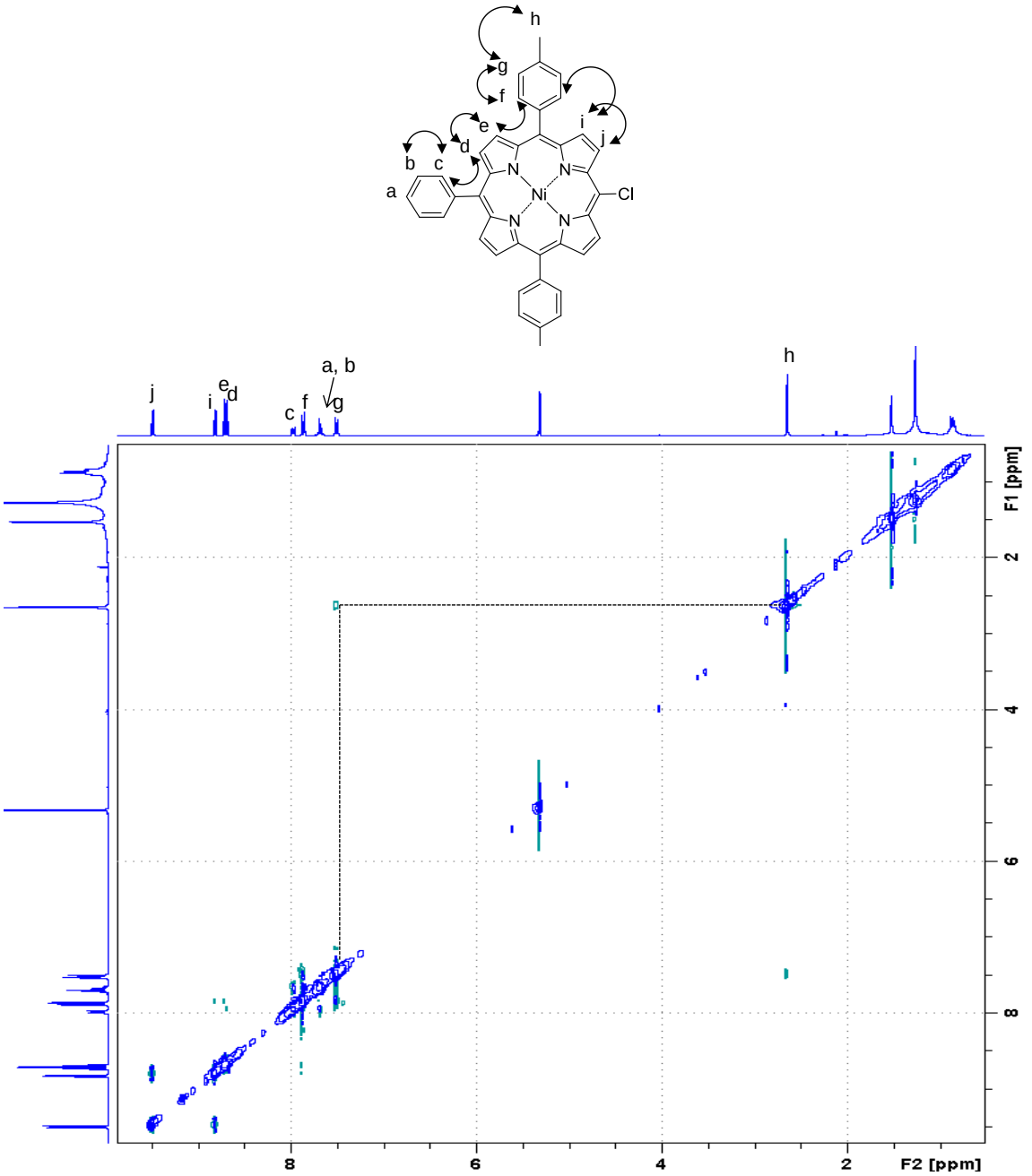

Fig. 17 ^{1}H-^{1}H NOESY NMR spectrum of **1-Ni-Cl** in CD_2Cl_2, 300 MHz, 300 K.

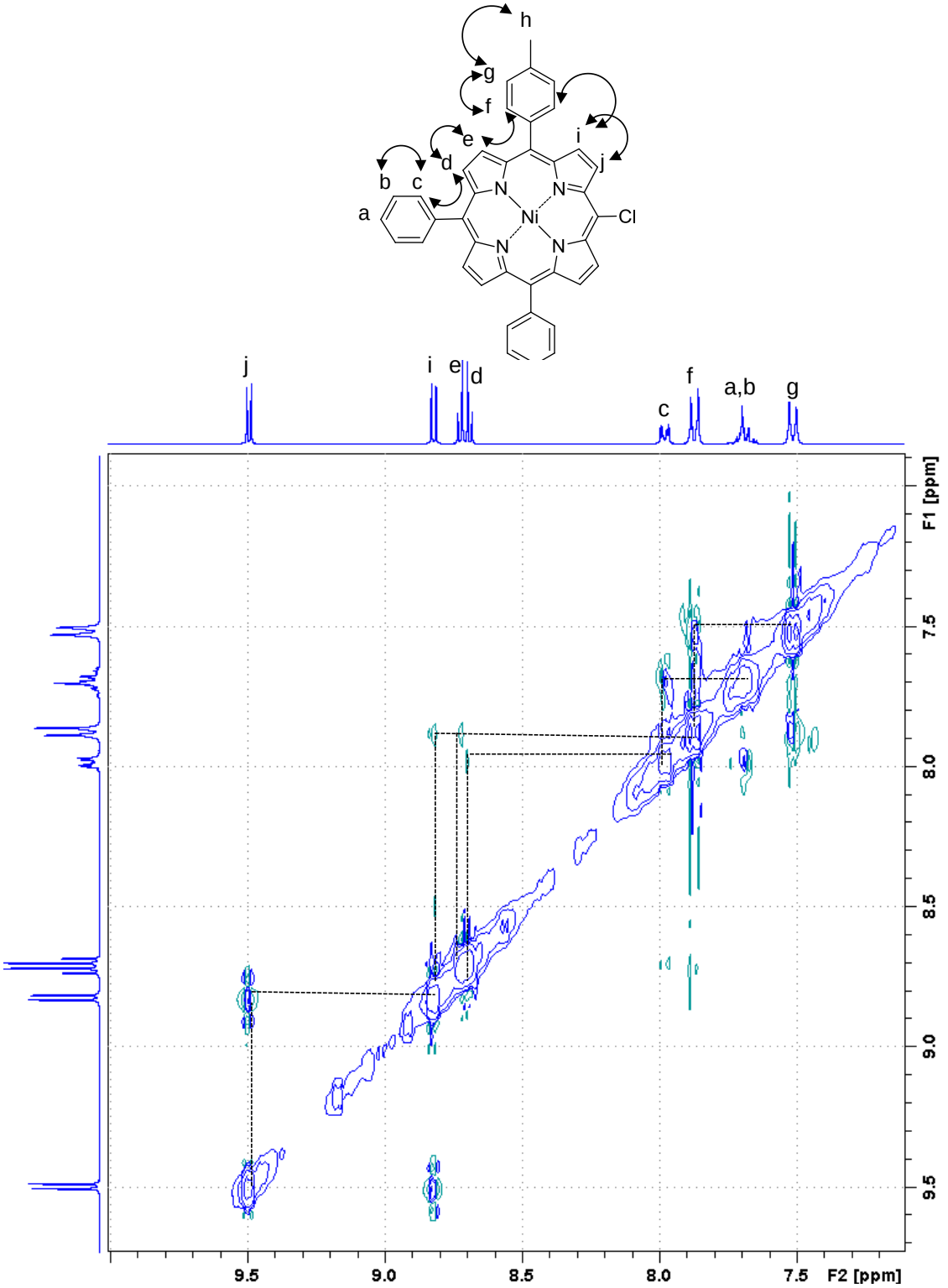

Fig. 18 Partial ^{1}H-^{1}H NOESY NMR spectrum of **1-Ni-Cl** in CD_2Cl_2, 300 MHz, 300 K.

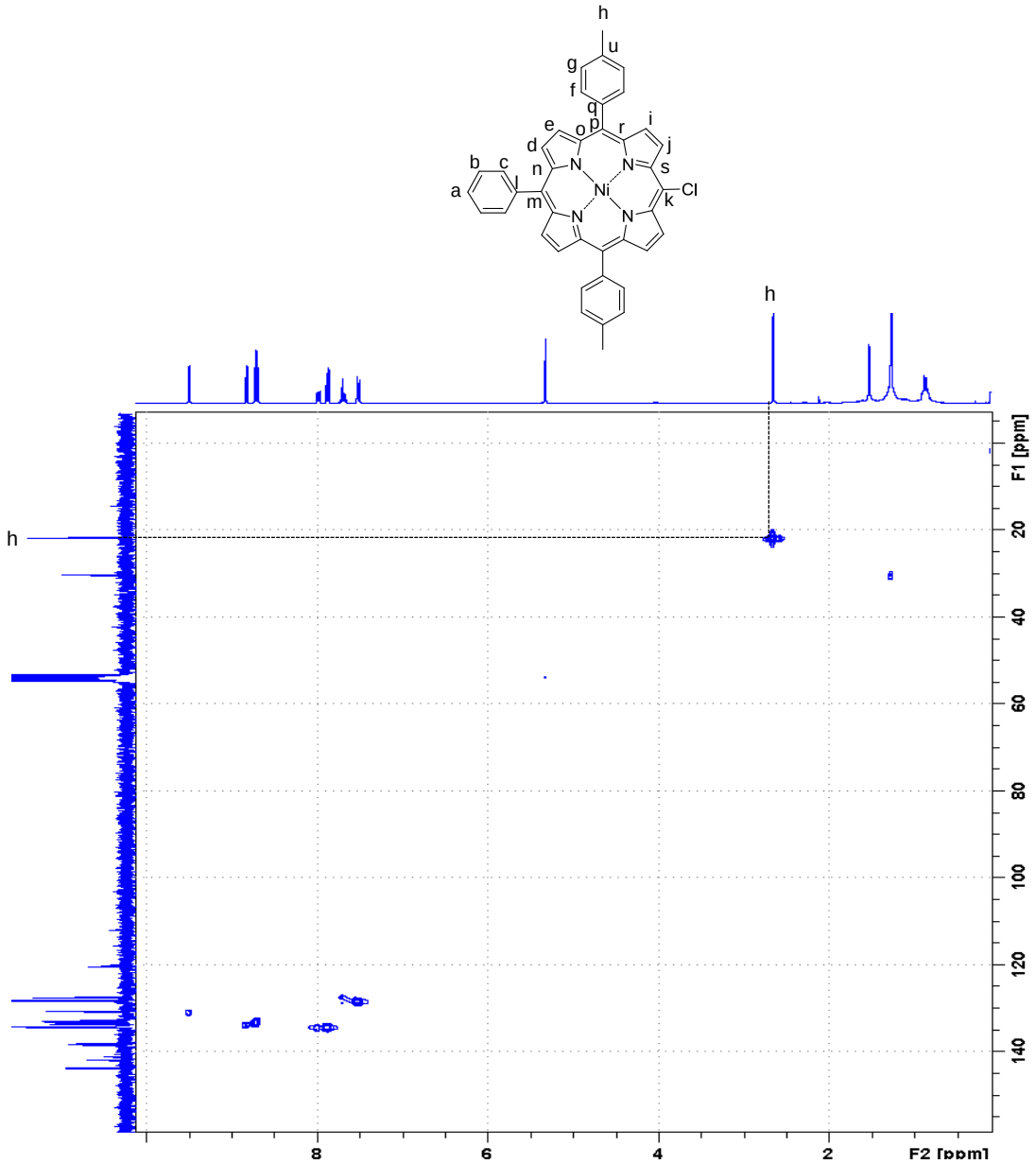

Fig. 19 ^{1}H-^{13}C HSQC NMR spectrum of **1-Ni-Cl** in CD_2Cl_2, 300 MHz, 300 K.

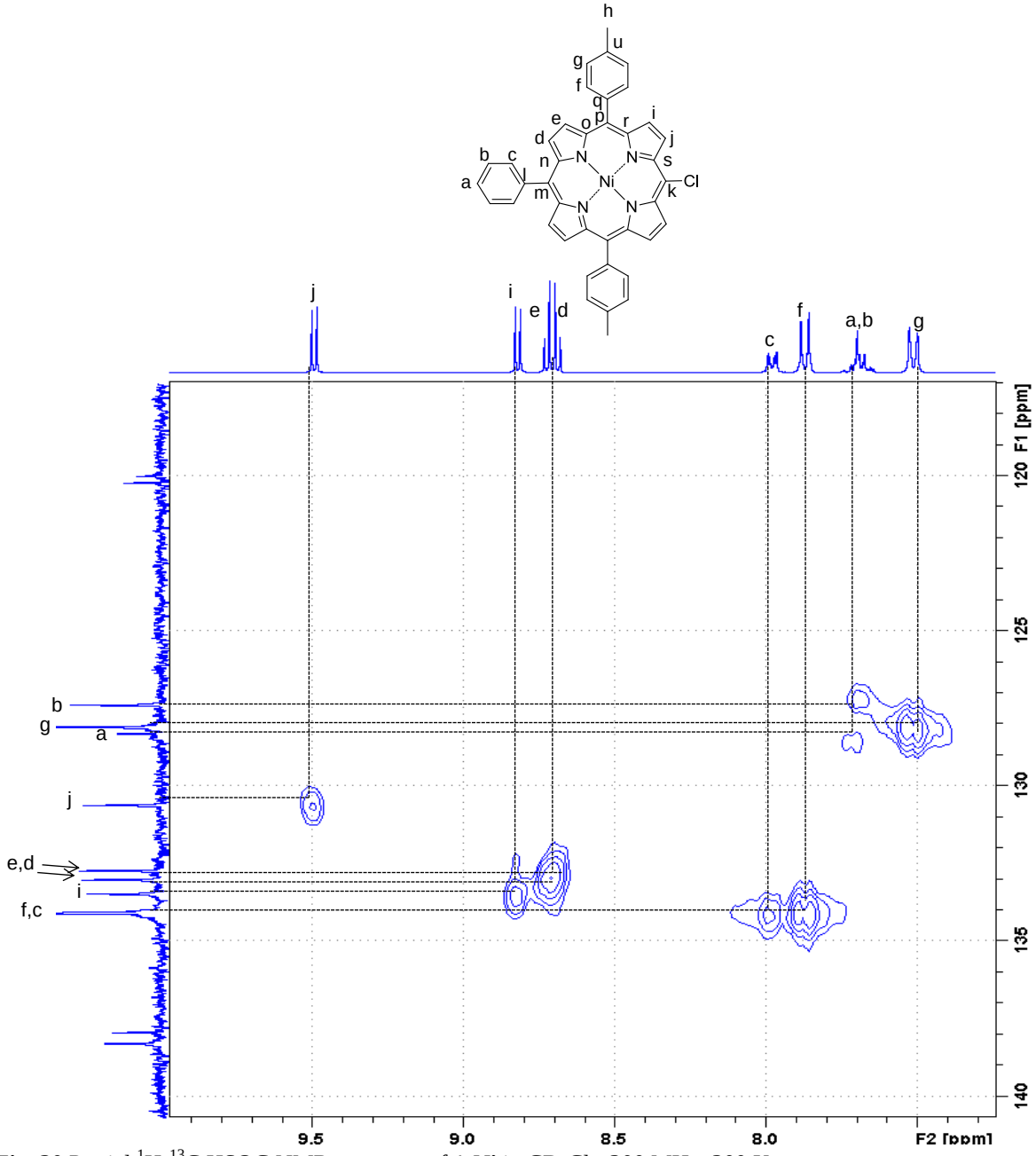

Fig. 20 Partial ^{1}H-^{13}C HSQC NMR spectrum of **1-Ni** in CD_2Cl_2, 300 MHz, 300 K.

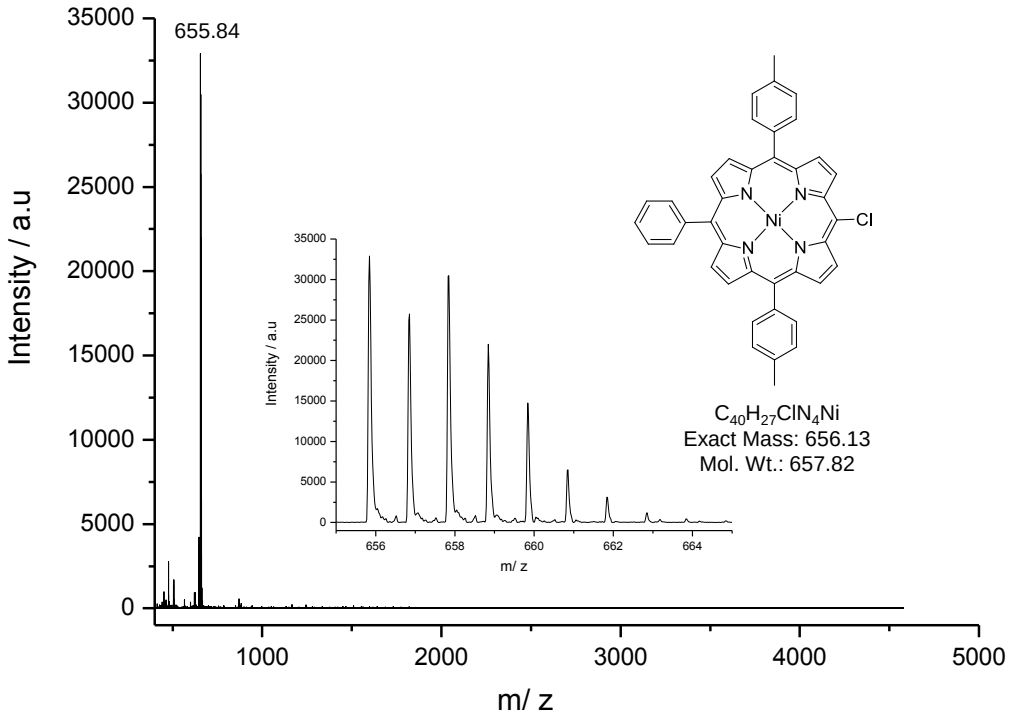

Fig. 21 MALDI-TOF mass spectrum of **1-Ni-Cl**.

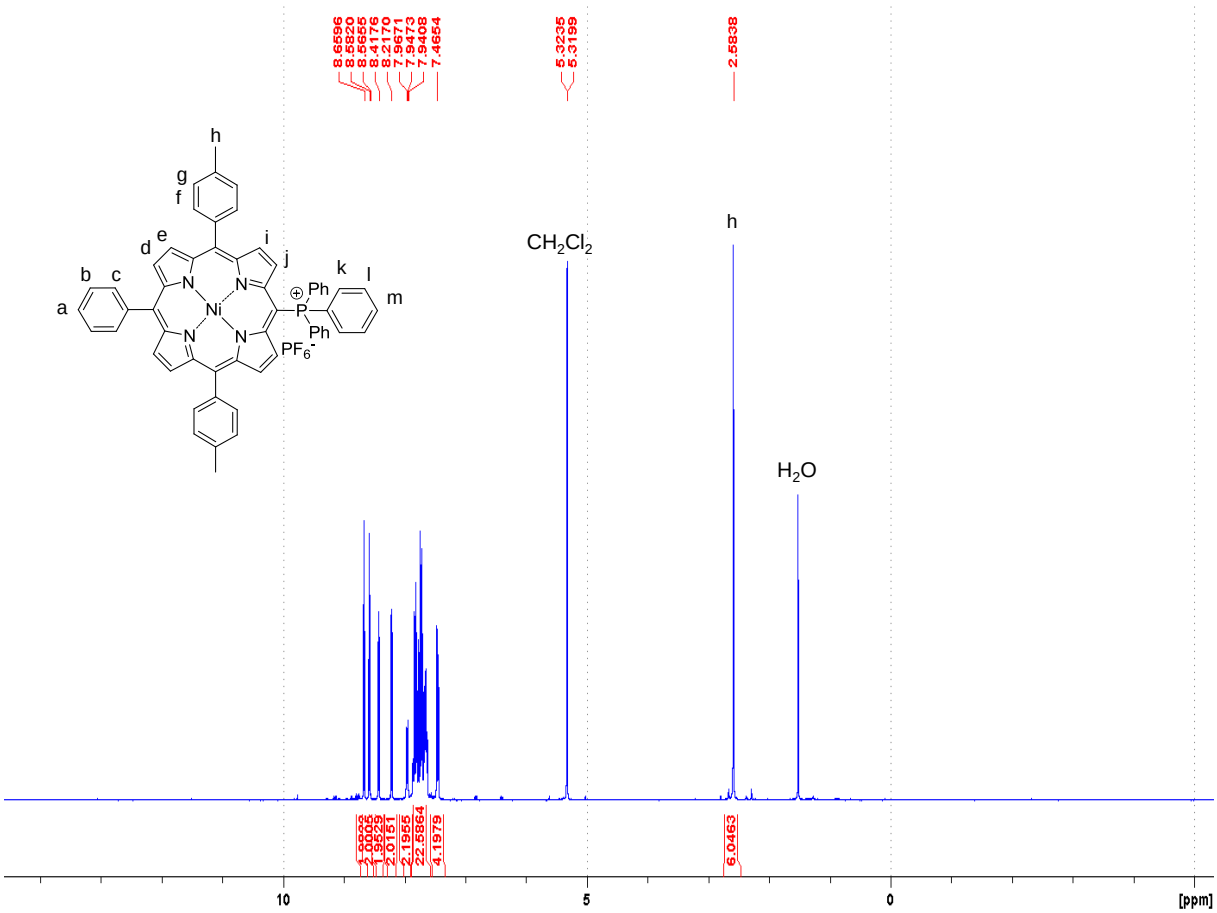

Fig. 22 ^{1}H NMR spectrum of **1-Ni-P**$^+$ in CD_2Cl_2, 300 MHz, 300 K.

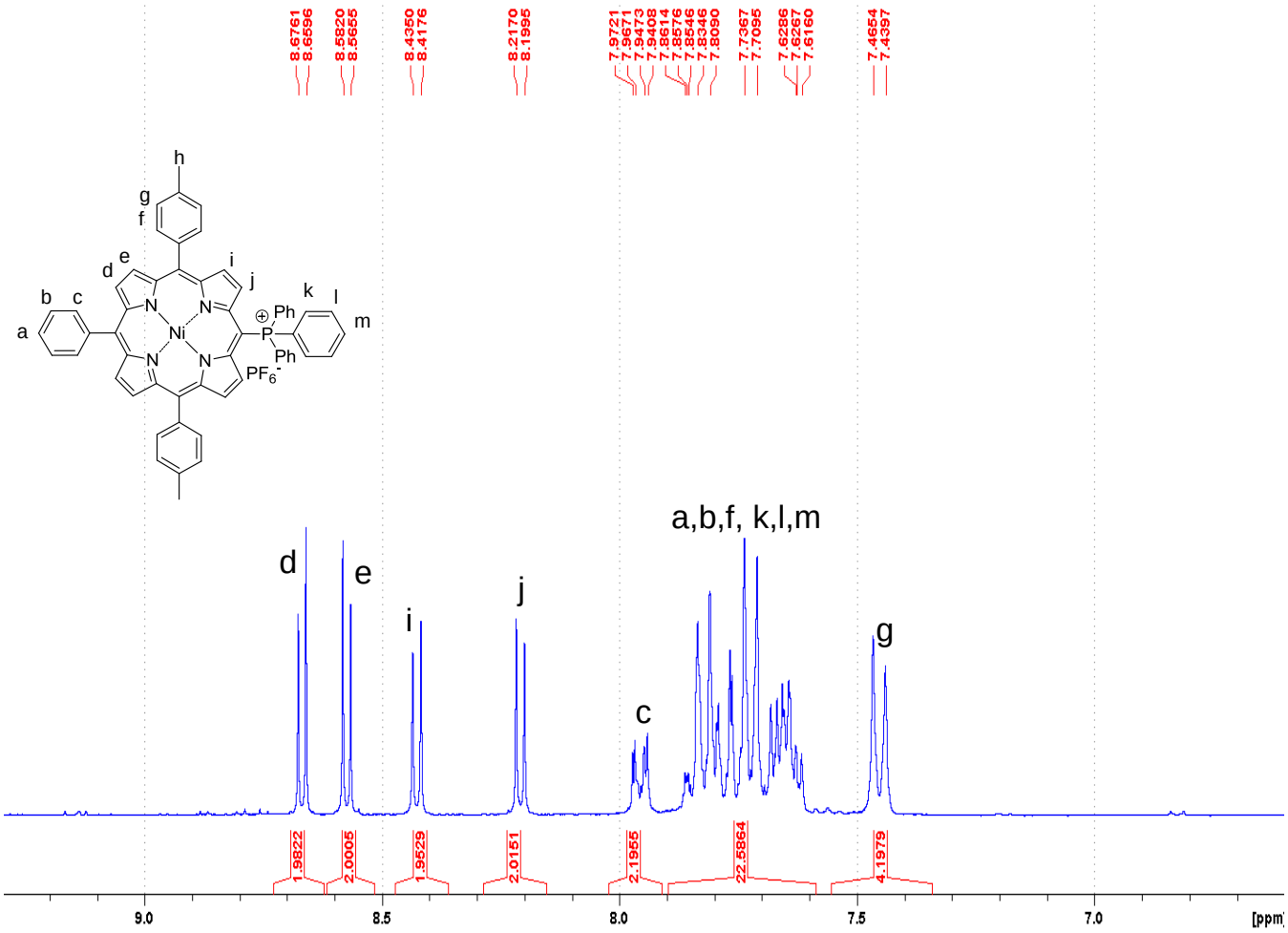

Fig. 23 Partial ^{1}H NMR spectrum of **1-Ni-P**$^{+}$ in CD_2Cl_2, 300 MHz, 300 K. δ (ppm) 2.58 (s, CH_3, 6H), 7.45 (d, ^{3}J = 7.7 Hz, *m*-Tol, 4H), 7.71-7.86 (m, *m*-and *p*-Ph, *o*-Tol, 22H), 7.94-7.97 (m, *o*-Ph, 2H), 8.21 (d, ^{3}J = 5.3 Hz, β-Pyrr, 2H), 8.43 (d, ^{3}J = 5.3 Hz, β-Pyrr, 2H), 8.57 (d, ^{3}J = 5,0 Hz, β-Pyrr, 2H), 8.67 (d, ^{3}J = 5,0 Hz, β-Pyrr, 2H).

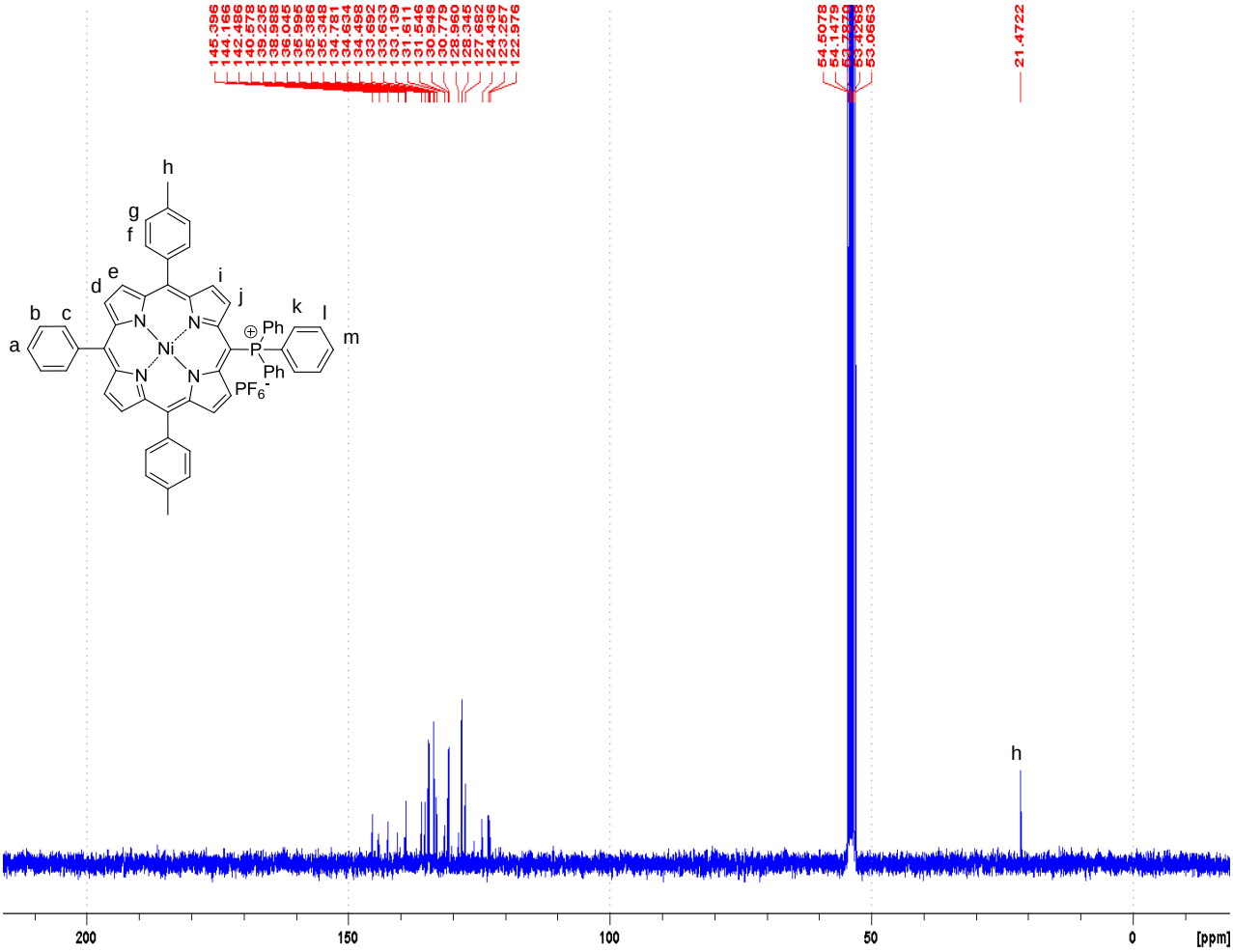

Fig. 24 ^{13}C NMR spectrum of **1-Ni-P**$^{+}$ in CD_2Cl_2, 75 MHz, 300 K.

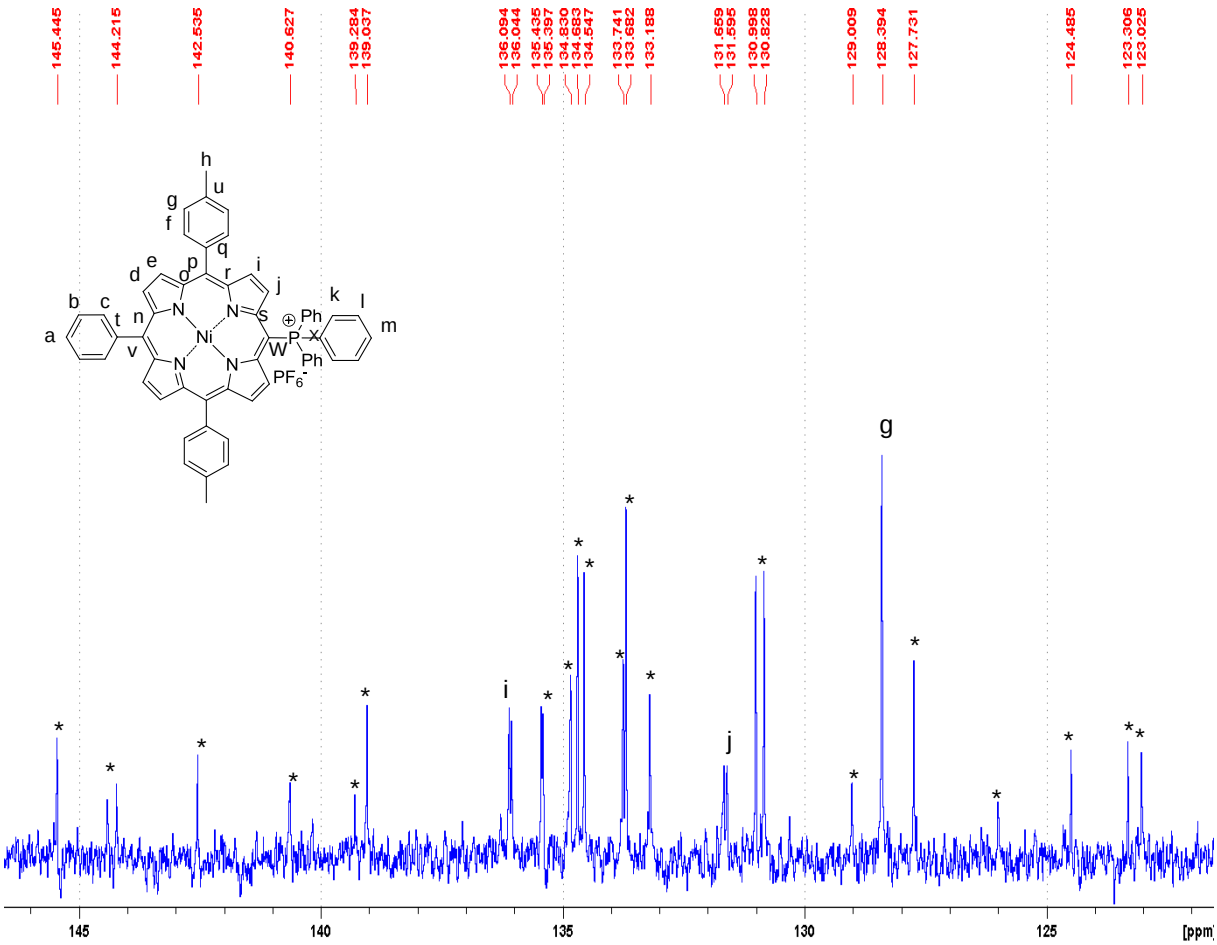

Fig. 25 Partial ^{13}C NMR spectrum of **1-Ni-P**$^{+}$ in CD_2Cl_2, 75 MHz, 300 K. (*): non attributed signals. These signals could be: a, b, c, d, e, f, k, l, m, n, o, p, q, u, r, s, t and v (these 19 C are uncoupled with proton signals in the ^{1}H-^{13}C HSQC experiment).

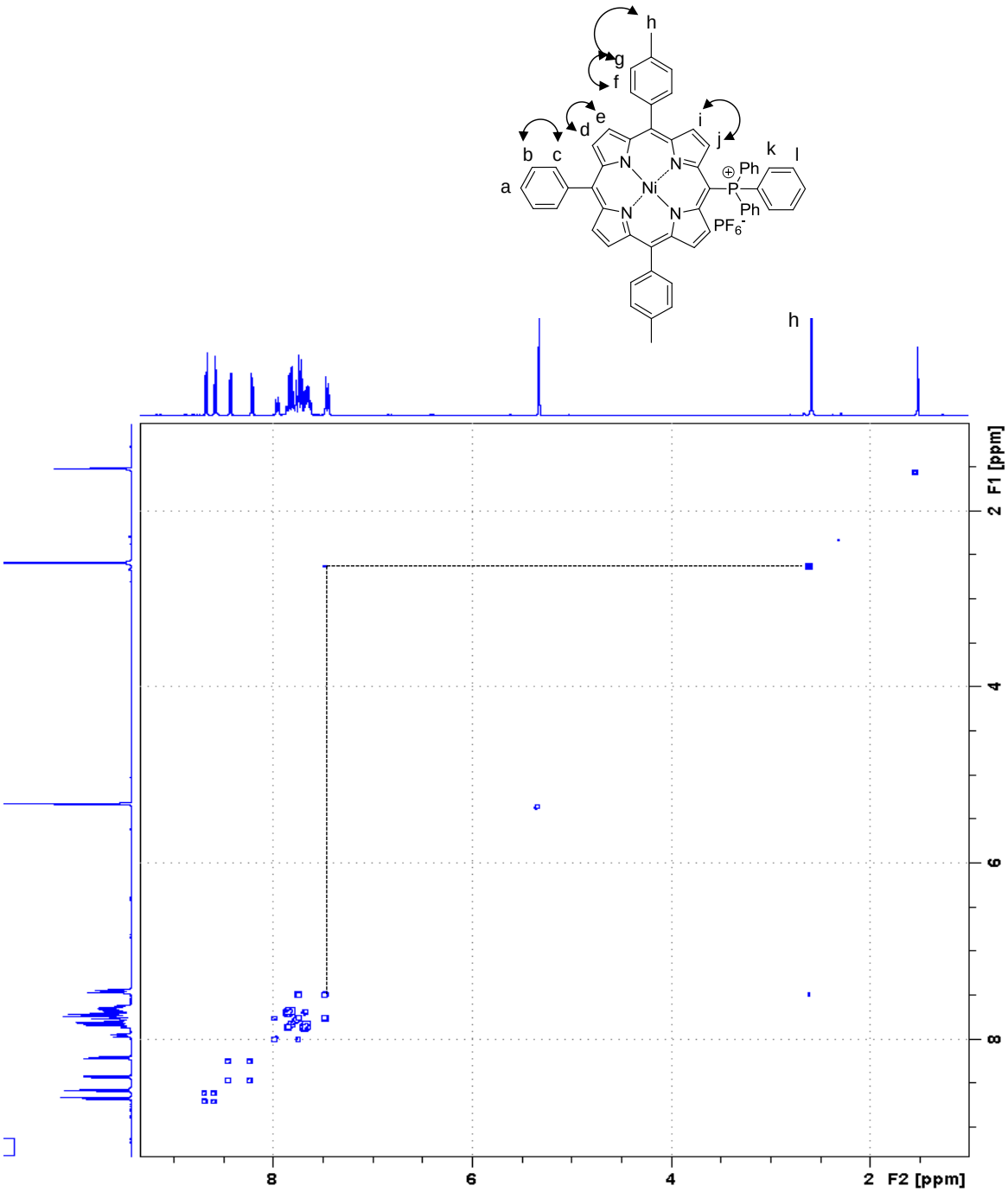

Fig. 26 ^{1}H-^{1}H COSY NMR spectrum of **1-Ni-P**$^{+}$ in CD_2Cl_2, 300 MHz, 300 K.

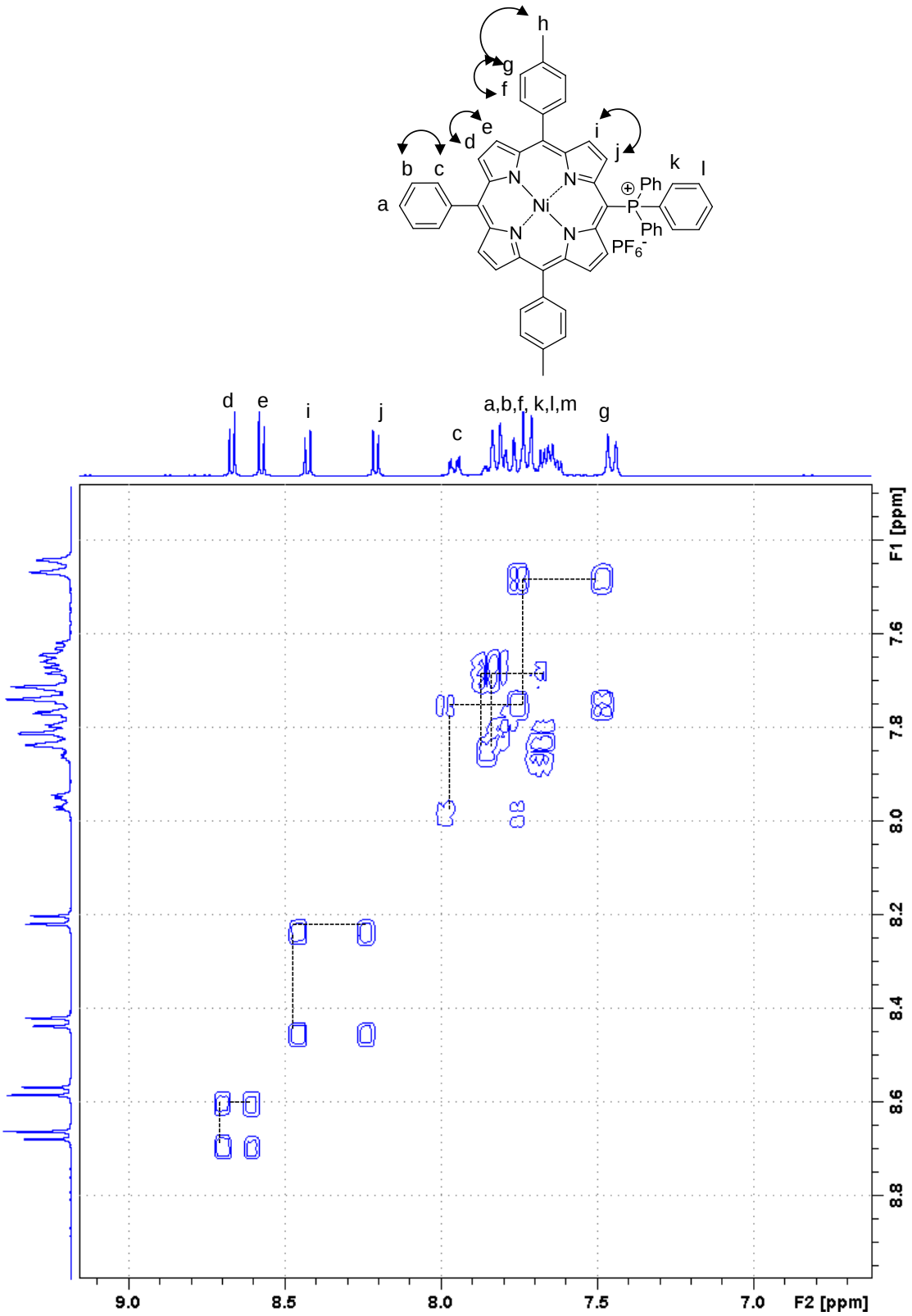

Fig. 27 Partial ^{1}H-^{1}H COSY NMR spectrum of **1-Ni-P**$^{+}$ in CD_2Cl_2, 300 MHz, 300 K.

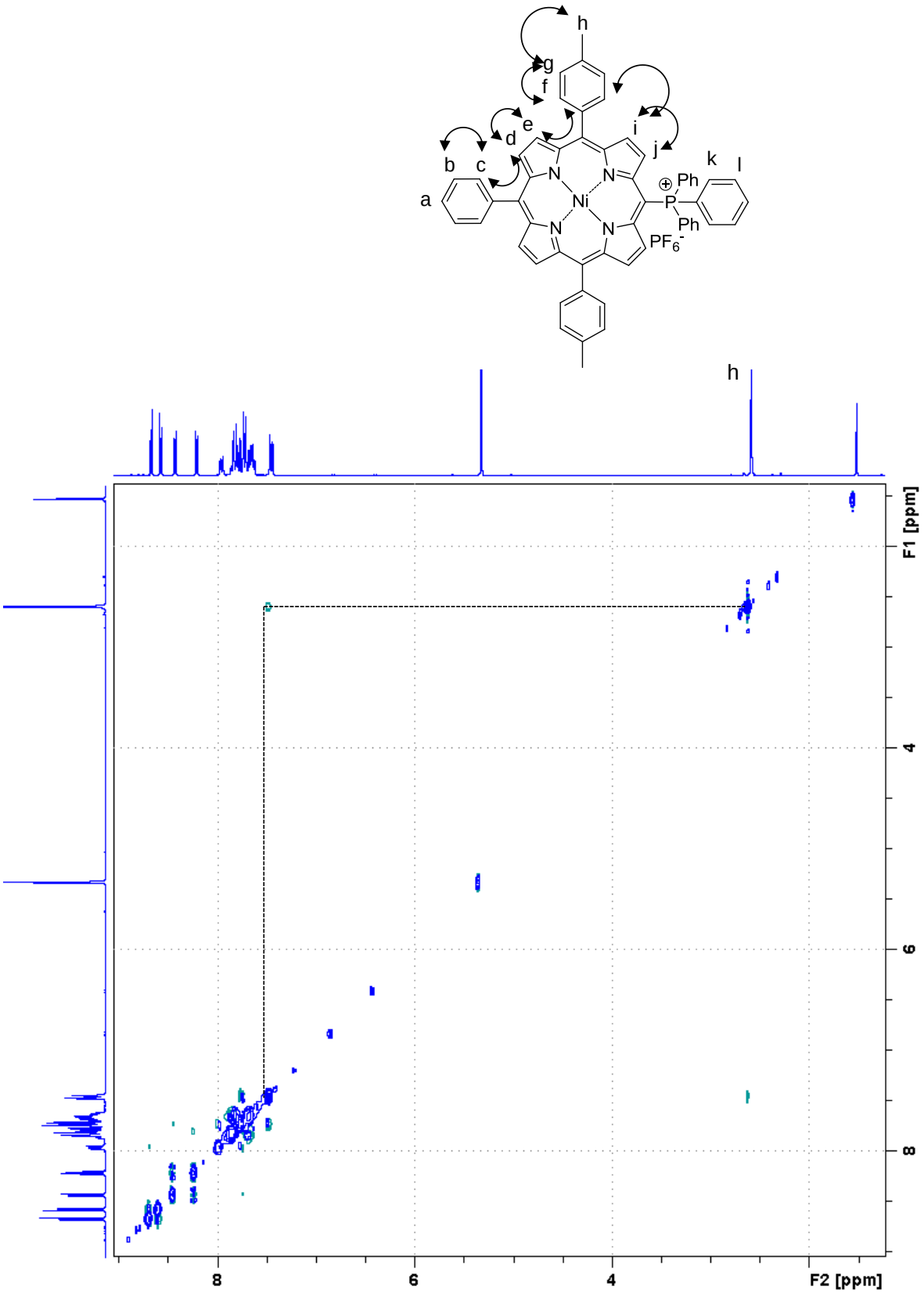

Fig. 28 ^{1}H-^{1}H NOESY NMR spectrum of **1-Ni-P**$^{+}$ in CD_2Cl_2, 300 MHz, 300 K.

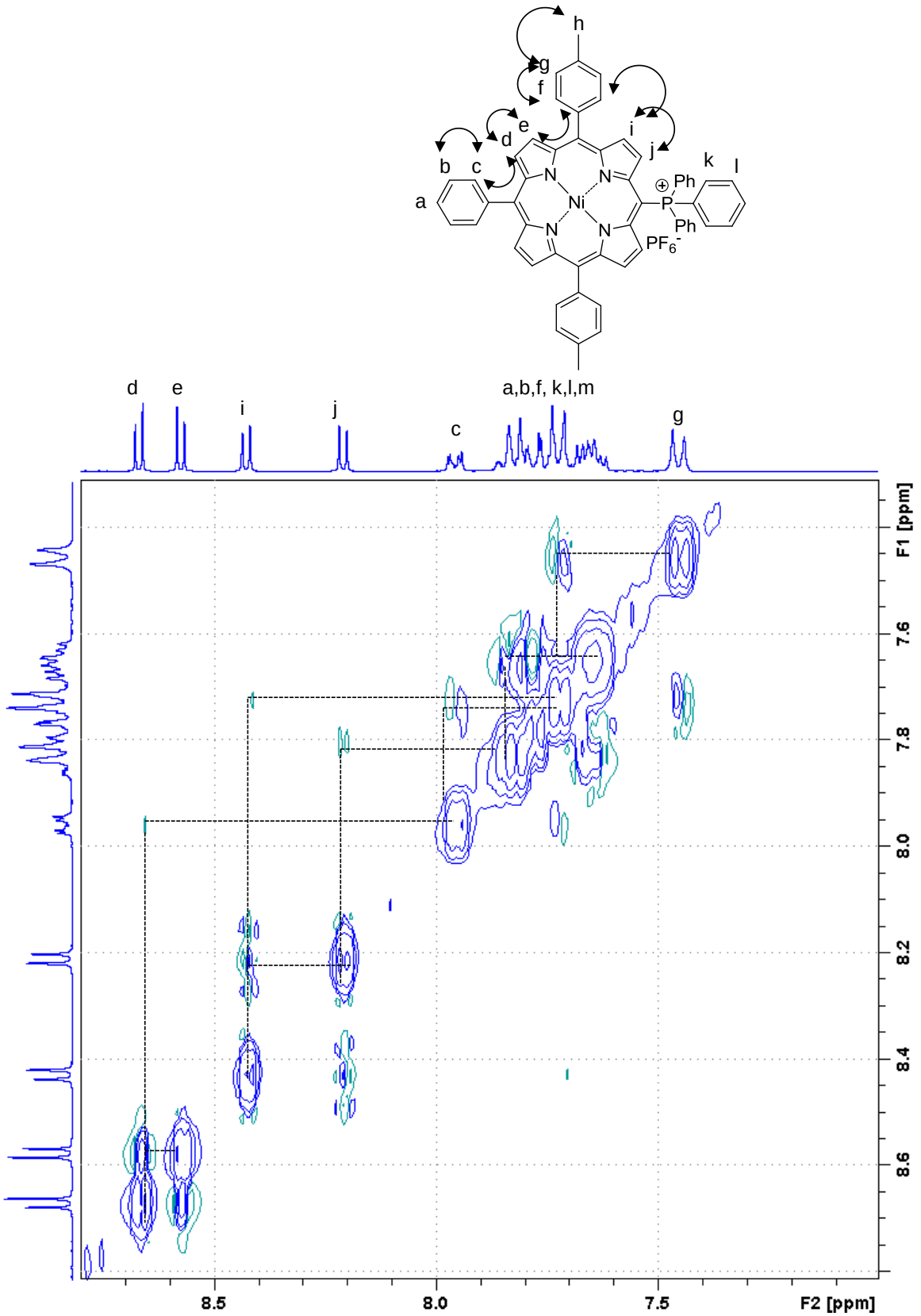

Fig. 29 Partial ^{1}H-^{1}H NOESY NMR spectrum of **1-Ni-P**$^{+}$ in CD_2Cl_2, 300 MHz, 300 K.

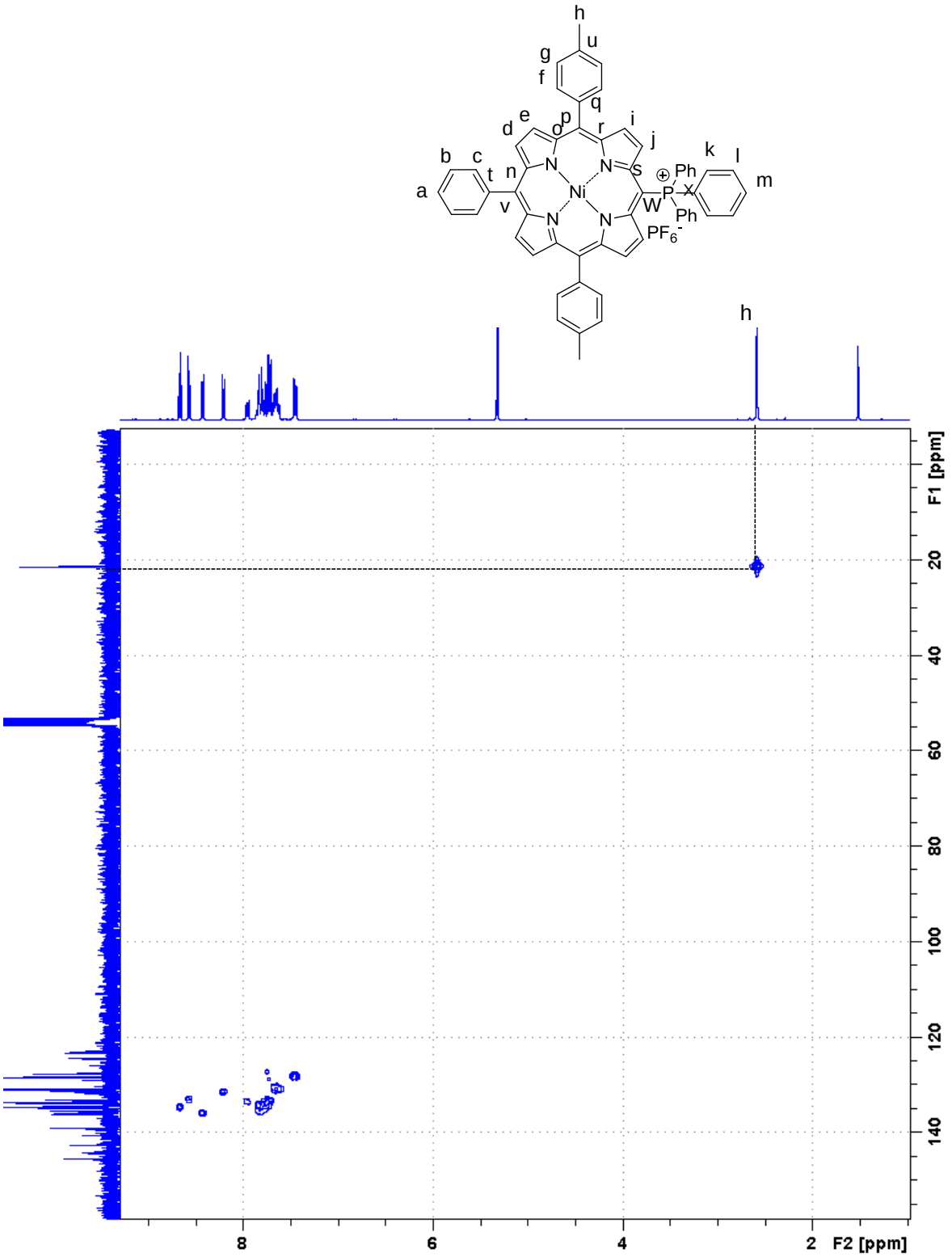

Fig. 30 ^{1}H-^{13}C HSQC NMR spectrum of **1-Ni-P**$^{+}$ in CD_2Cl_2, 300 MHz, 300 K.

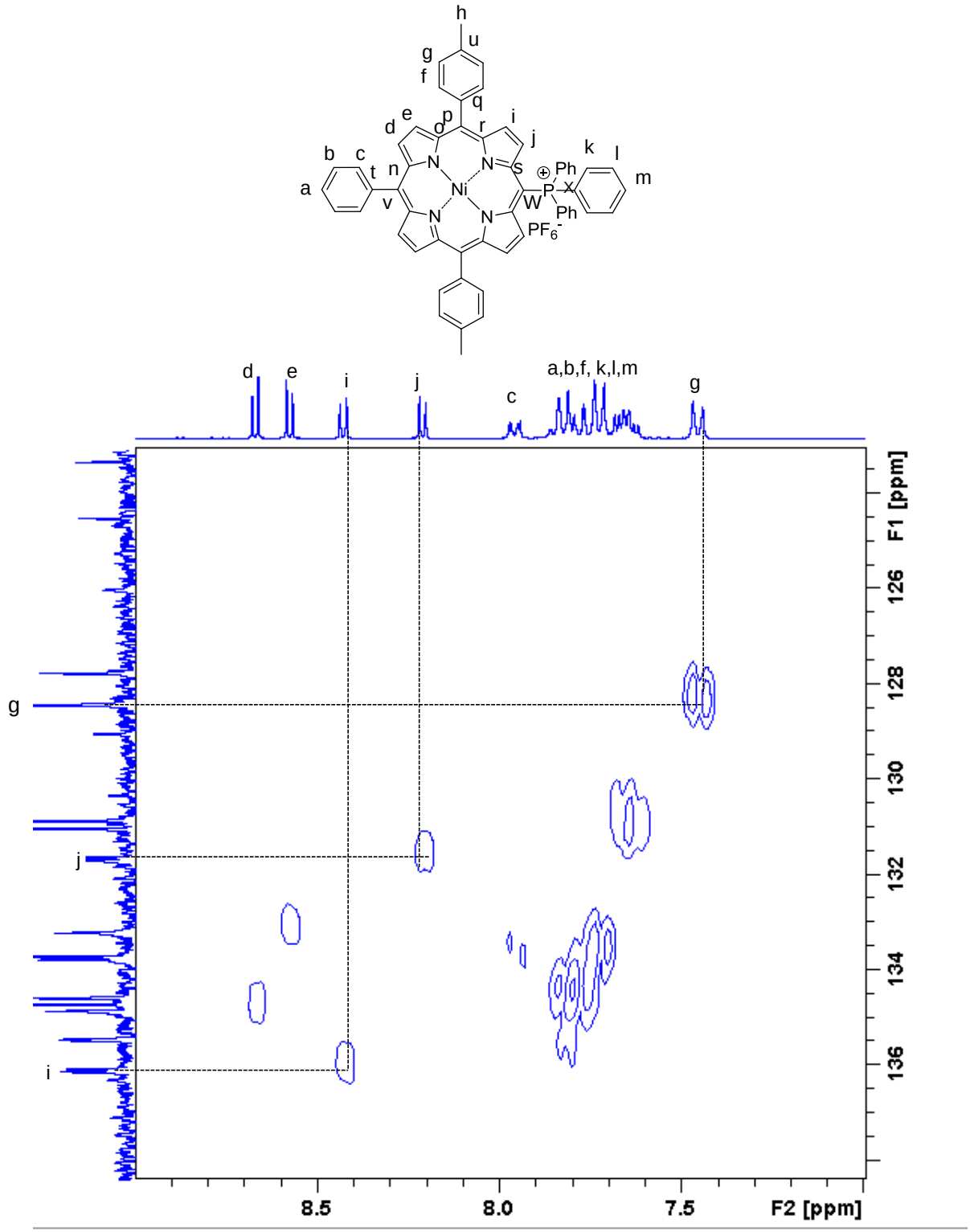

Fig. 31 Partial ^{1}H-^{13}C HSQC NMR spectrum of **1-Ni-P**$^{+}$ in CD_2Cl_2, 300 MHz, 300 K.

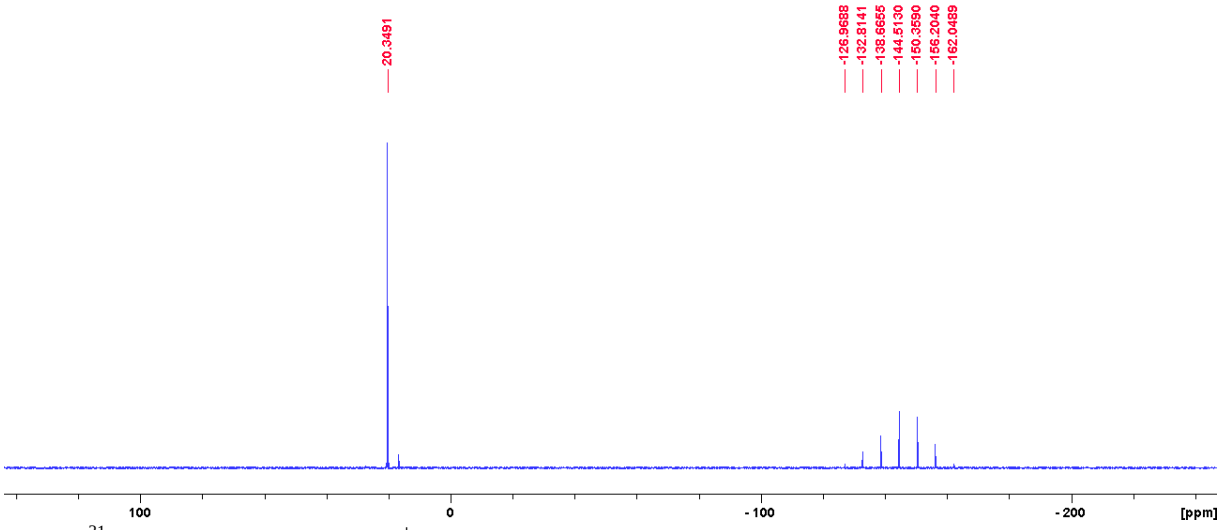

Fig. 32 ^{31}P NMR spectrum of **1-Ni-P**$^{+}$ in CD_2Cl_2, 121 MHz, 300 K.

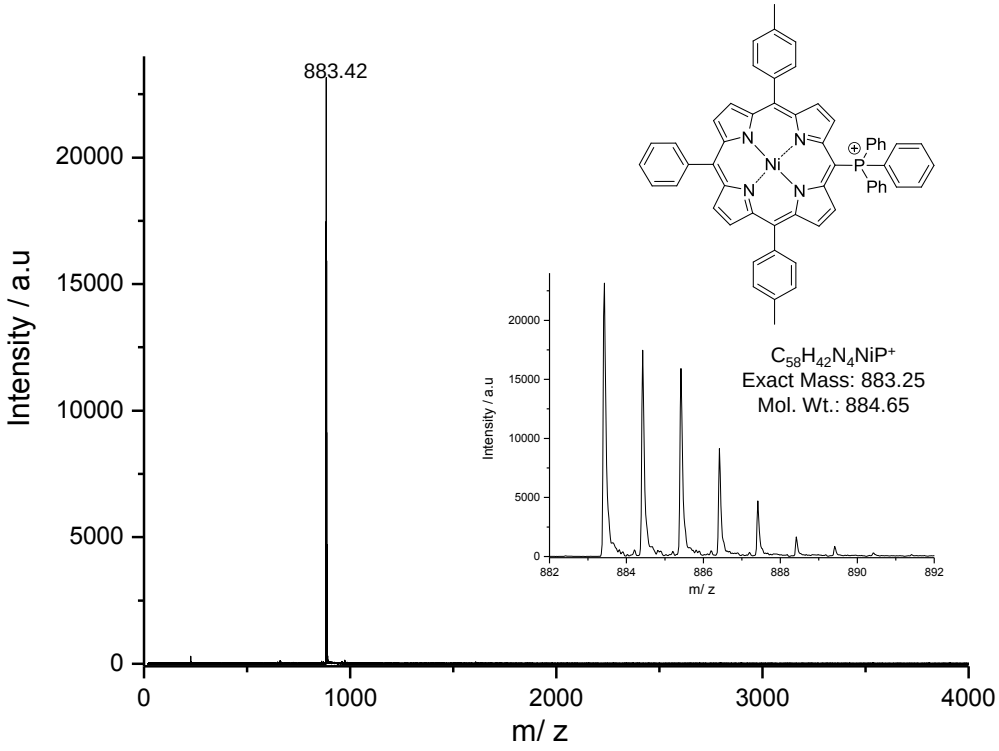

Fig. 33 MALDI-TOF mass spectrum of **1-Ni-P**$^{+}$.

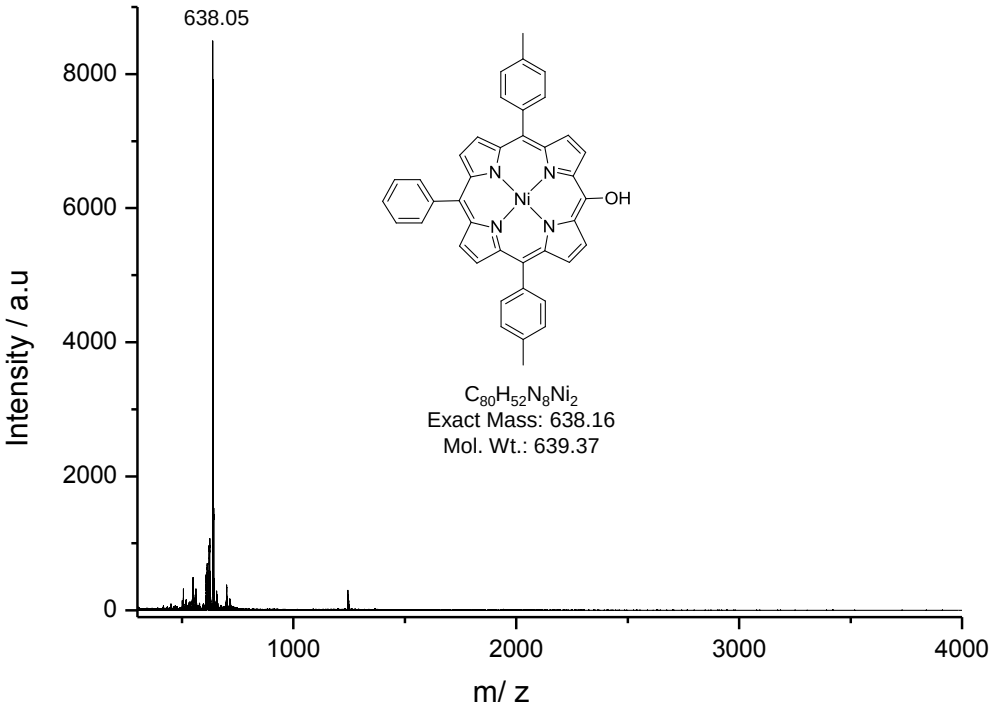

Fig. 34 MALDI-TOF mass spectrum of a crude solution resulting from electrolysis of **1-Ni** in DMF 0.1 $TEAPF_6$; E_{app} = 1.10 V *vs.* SCE, −5.5 e, 3 compartments, working electrode: Pt spiral.

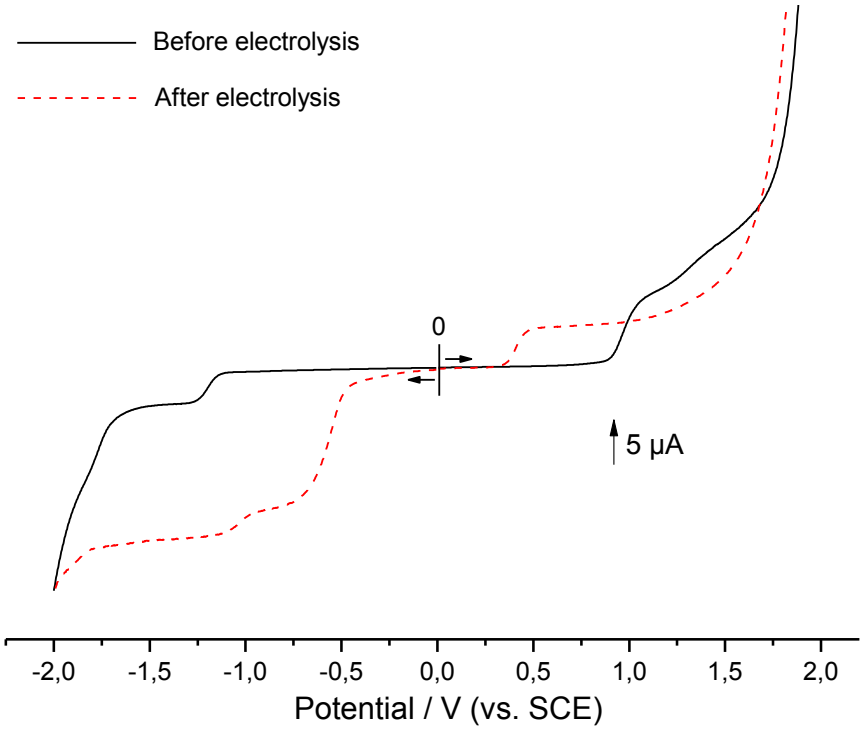

Fig. 35 RDE voltammograms before (black/solid line) and after (red/dashed line) electrolysis of **1-Ni** in DMF containing 0.1 M $TEAPF_6$ in the conditions of Fig. 34 (WE: Pt, Ø = 2 mm, 10 mV s^{-1}, ω = 500 rpm, [1-Ni] = 5.0×10^{-4} M).

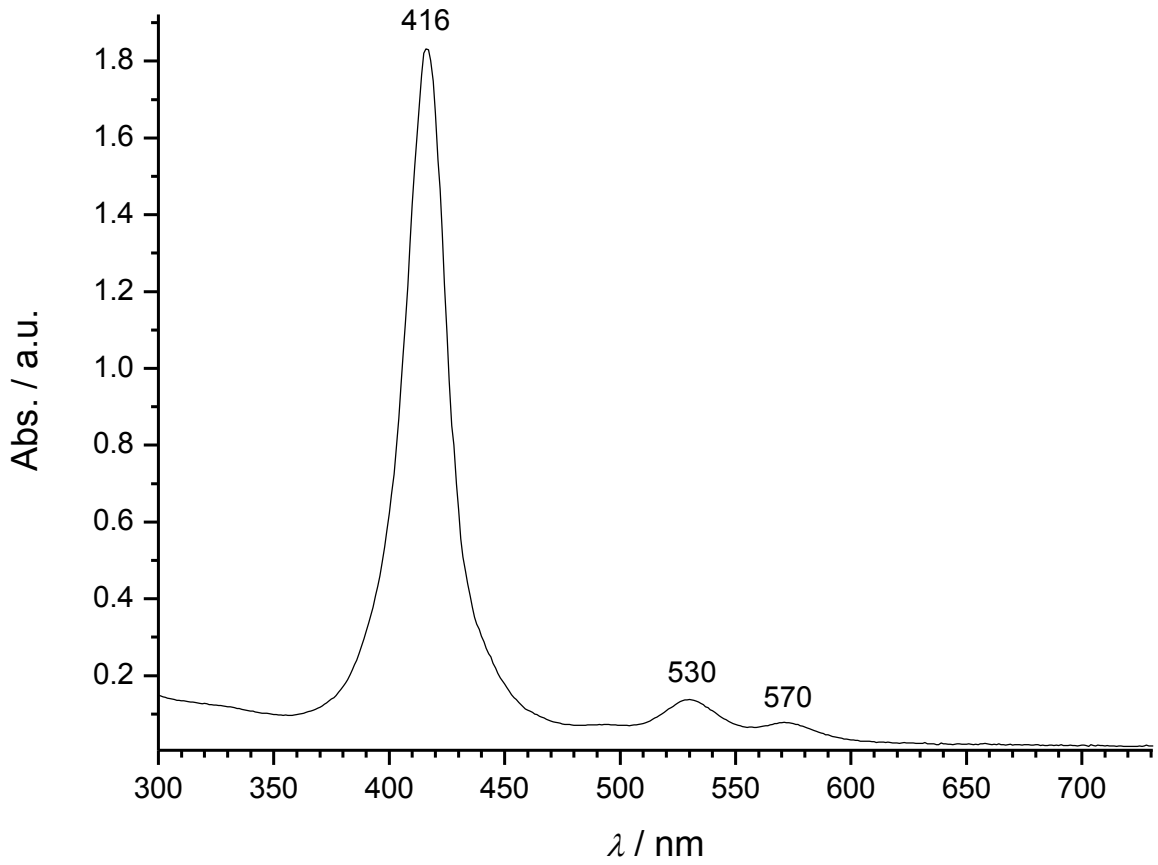

Fig. 36 UV-Vis absorption spectrum of the diluted crude solution (in CH_2Cl_2) resulting from electrolysis of **1-Ni** in DMF 0.1 $TEAPF_6$; E_{app} = 1.10 V *vs*. SCE, −5.5 e, 3 compartments, working electrode: Pt spiral.

*Synthesis of **3-Ni***

After dissolution of **1-Ni** (19.5 mg, 31.28 μmol) in 15 mL of dichloroethane, a mixture of $AuCl_3$ (10.1 mg, 33.3 μmol) and AgOTf (50.0 mg, 0.19 mmol) was added at room temperature under argon. The reaction mixture was stirred for 3 min and was quenched immediately with saturated $NaHCO_3$ aqueous solution (10 mL) and stirred for additional 5 min. The organic layer was washed with 4×250 ml of distilled water. After evaporation of the solvent, the crude product was purified by column chromatography on silica gel (CH_2Cl_2), affording **3-Ni** (17.5 mg, 14.11 μmol, 89.7% yield).

λ_{max} (CH_2Cl_2)/nm (relative absorbance/ %) = 415 (100), 499 (64.64), 543 (67.55), 755 (52.24).

*Synthesis of **2-Ni***

1-Ni (30.0 mg, 48.12 μmol) was dissolved in 15 mL of $CHCl_3$. 2.2 eq. of PIFA was then added and the reaction mixture was stirred for 15 min at room temperature. The solution was washed with 4×250 ml of distilled water. After evaporation of the solvent, the crude product was purified by column chromatography on silica gel (CH_2Cl_2), affording **2-Ni** (11.9 mg, 40% yield).

λ_{max} (CH_2Cl_2)/nm (relative absorbance %)= 414 (95), 446 (100), 536 (26.89).

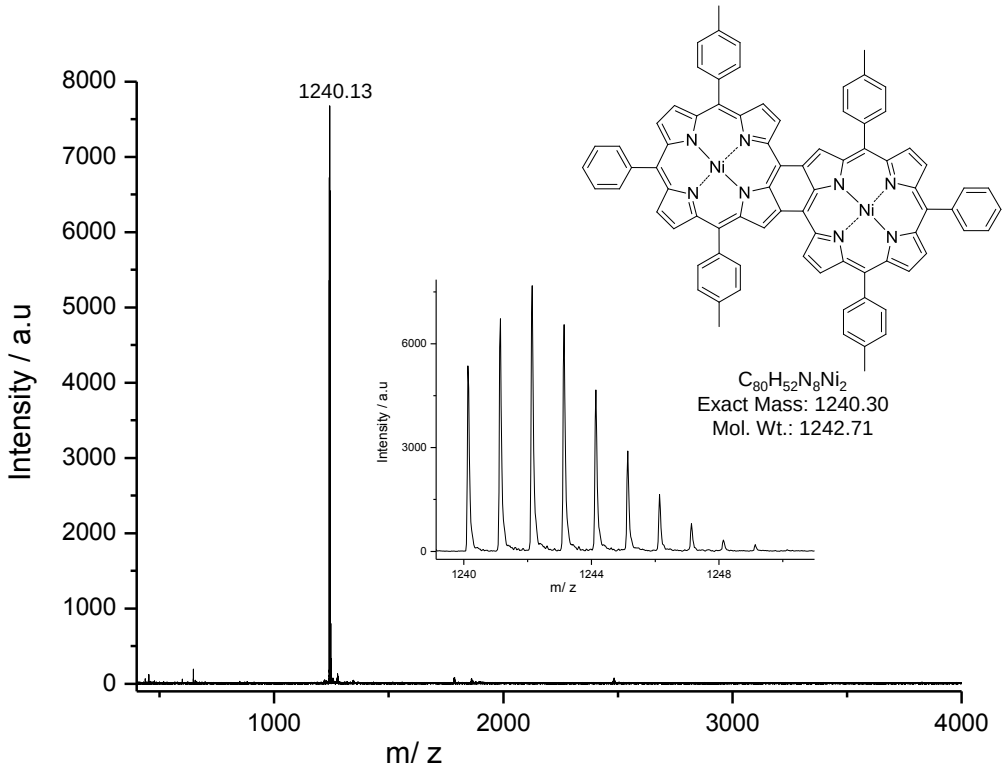

Fig. 37 MALDI-TOF mass spectrum of **3-Ni**.

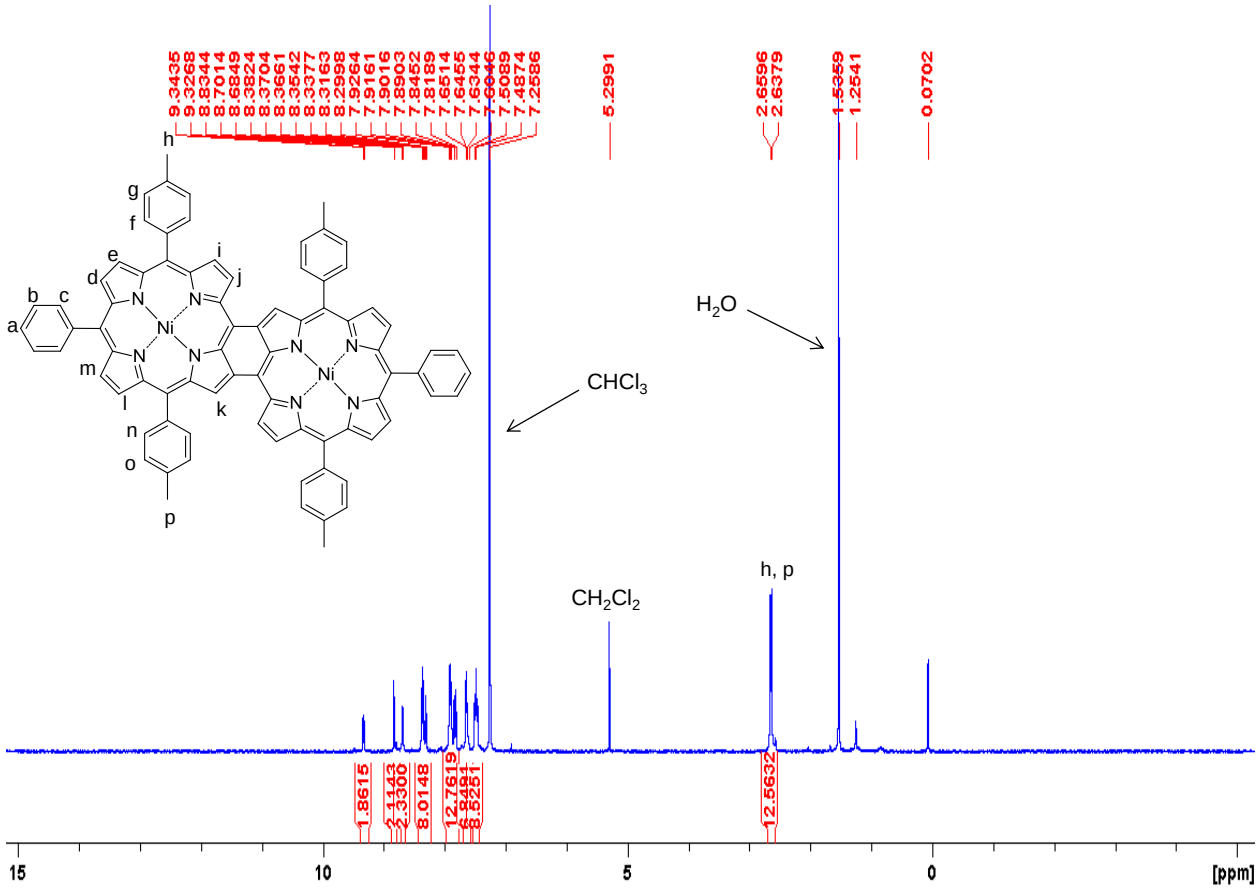

Fig. 38 ^{1}H NMR spectrum of **3-Ni** in $CDCl_3$, 300 MHz, 300 K.

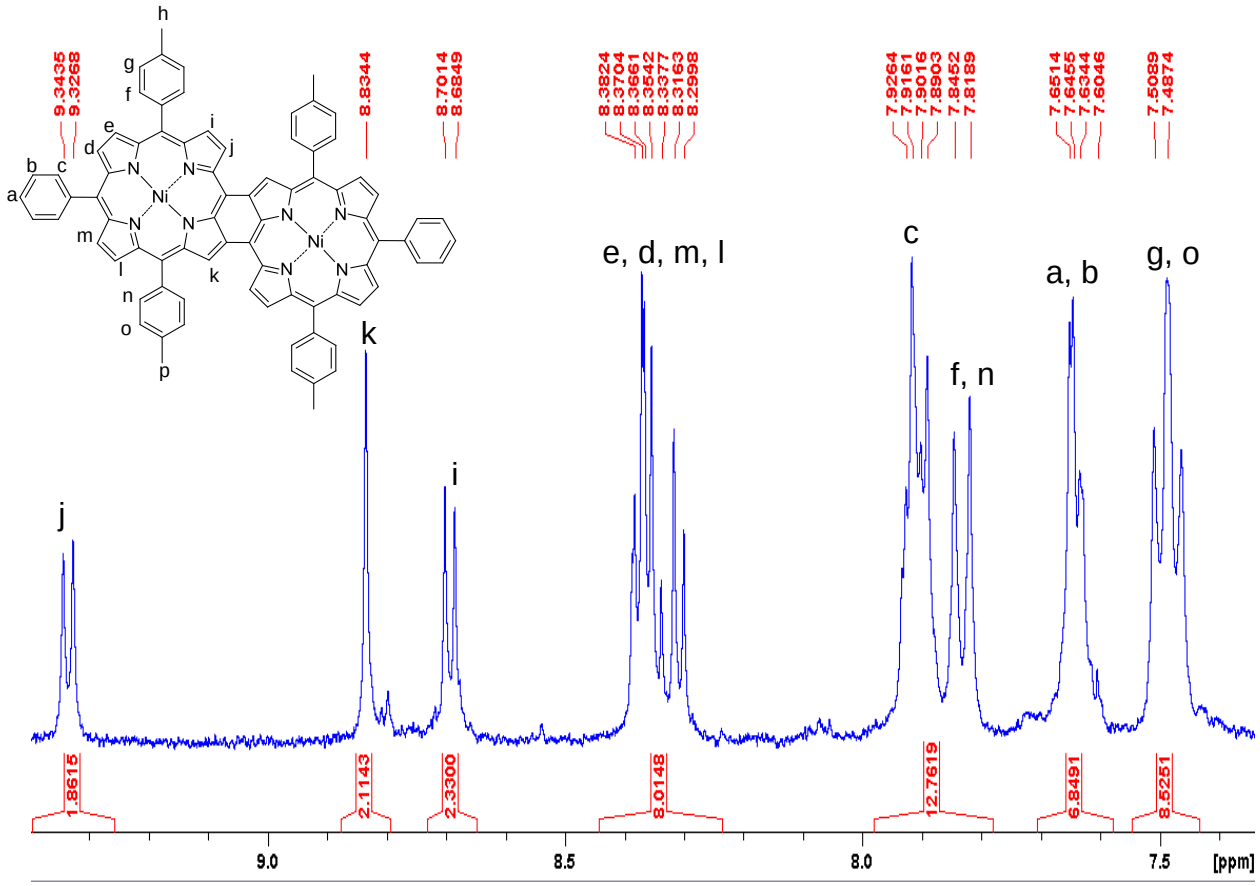

Fig. 39 Partial ^{1}H NMR spectrum of **3-Ni** in $CDCl_3$, 300 MHz, 300 K. δ (ppm) 2.64 (s, CH_3, 12H), 7.49 (m, ^{3}J = 7.7 Hz, *m*-tol, 8H), 7.61-7.69 (m, *m*-and *p*-Ph, 6H), 7.83 (d, ^{3}J = 7.9 Hz, *o*-tol, 8H), 7.86-7.96 (m, *o*-Ph, 4H), 8.28-8.41 (m, *β*-Pyrr, 8H), 8.69 (d, ^{3}J = 5.0 Hz, *β*-Pyrr, 2H), 8.83 (s, *β*-Pyrr, 2H), 9.34 (d, ^{3}J = 5.0 Hz, *β*-Pyrr, 2H).

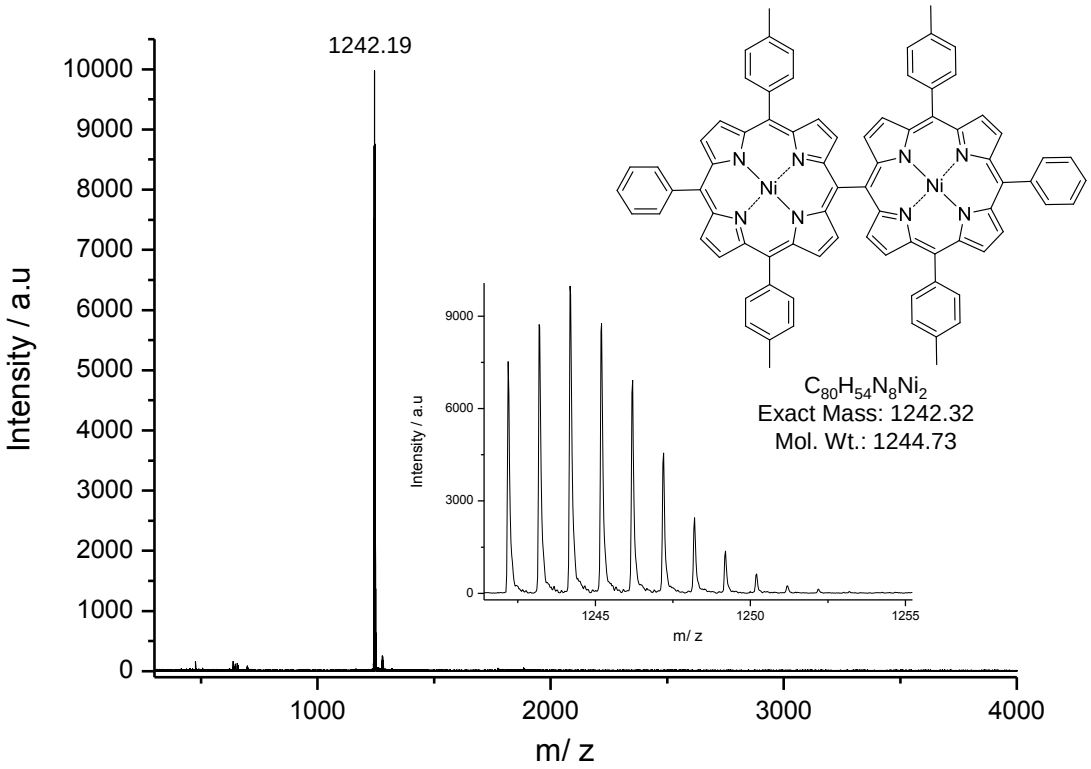

Fig. 40 MALDI-TOF mass spectrum of **2-Ni**.

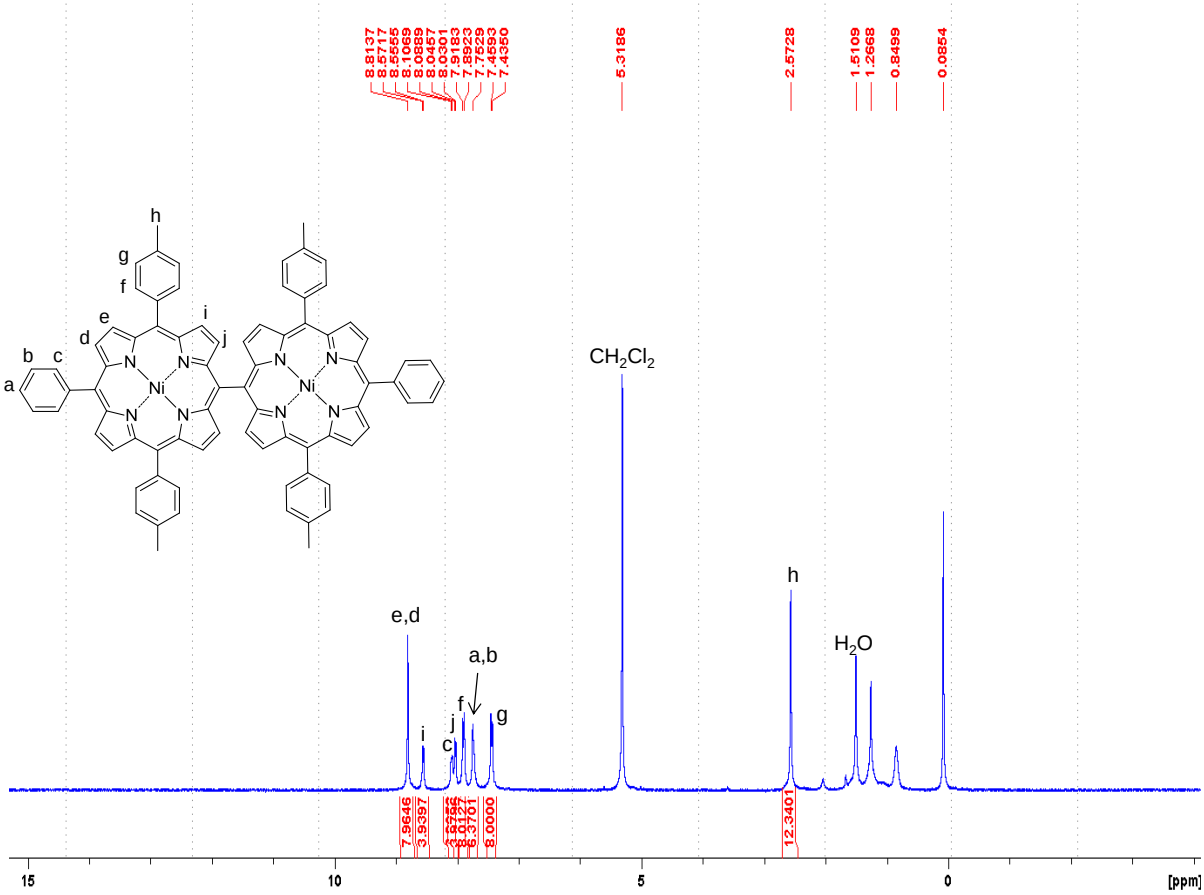

Fig. 41 ^{1}H NMR spectrum of **2-Ni** in CD_2Cl_2, 300 MHz, 300 K.

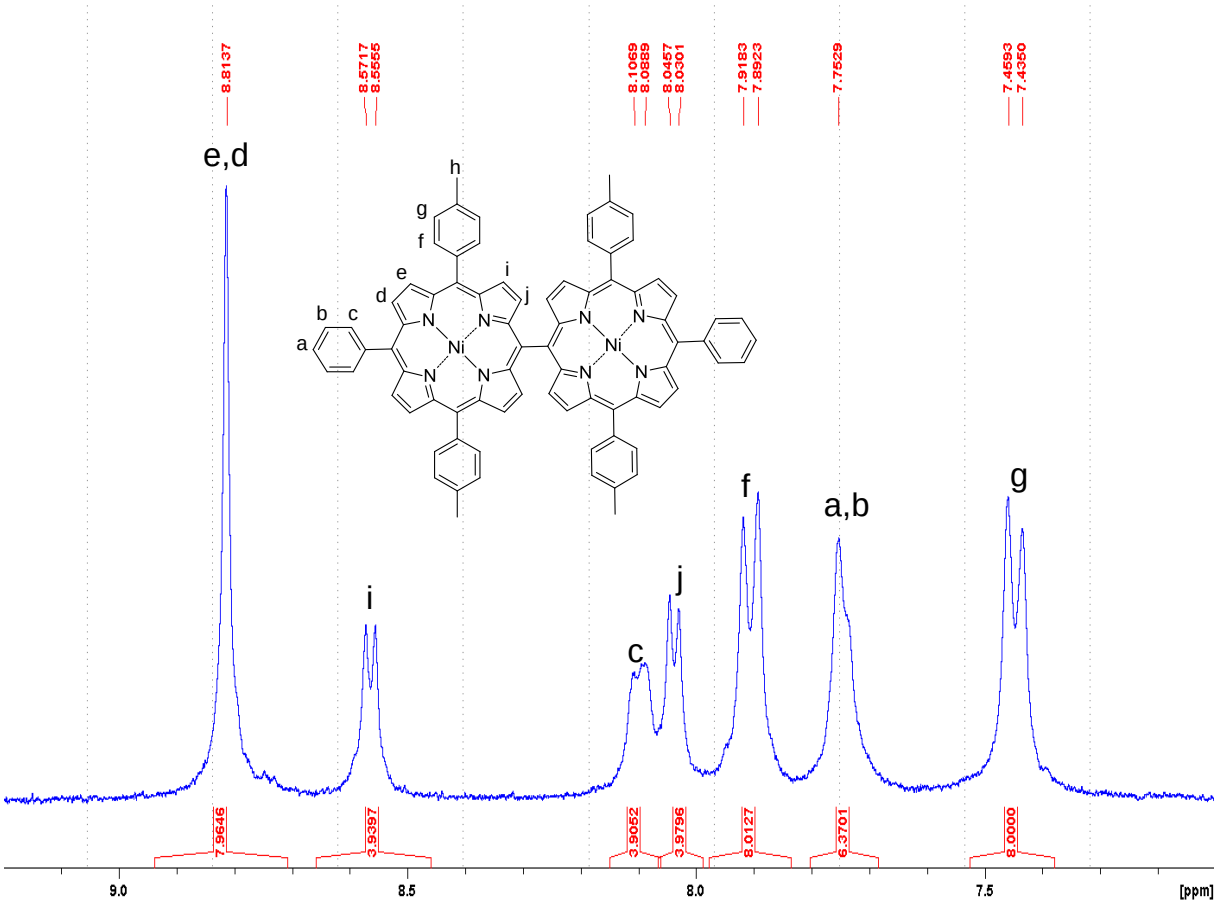

Fig. 42 Partial ^{1}H NMR spectrum of **2-Ni** in CD_2Cl_2, 300 MHz, 300 K. δ (ppm) 2.57 (s, CH_3, 12H), 7.45 (d, ^{3}J = 7.3 Hz, *m*-tol, 8H), 7.69-7.81 (m, *m*-and *p*-Ph, 6H), 7.90 (d, ^{3}J = 7.8 Hz, *o*-tol, 8H), 8.04 (d, ^{3}J = 4.7 Hz, β-Pyrr, 4H) 8.06-8.18 (m, *o*-Ph, 4H), 8.56 (d, ^{3}J = 4.9 Hz, β-Pyrr, 4H), 8.81 (s, β-Pyrr, 8H).

*Synthesis of **2'-Ni***

2'-Ni was synthesized according to reference [1]. Despite all our effort, perfect purification of this compound by column chromatography (CH_2Cl_2/*n*-heptane 20/80) was impossible but its purity can be estimated higher than 80% by NMR spectroscopy.

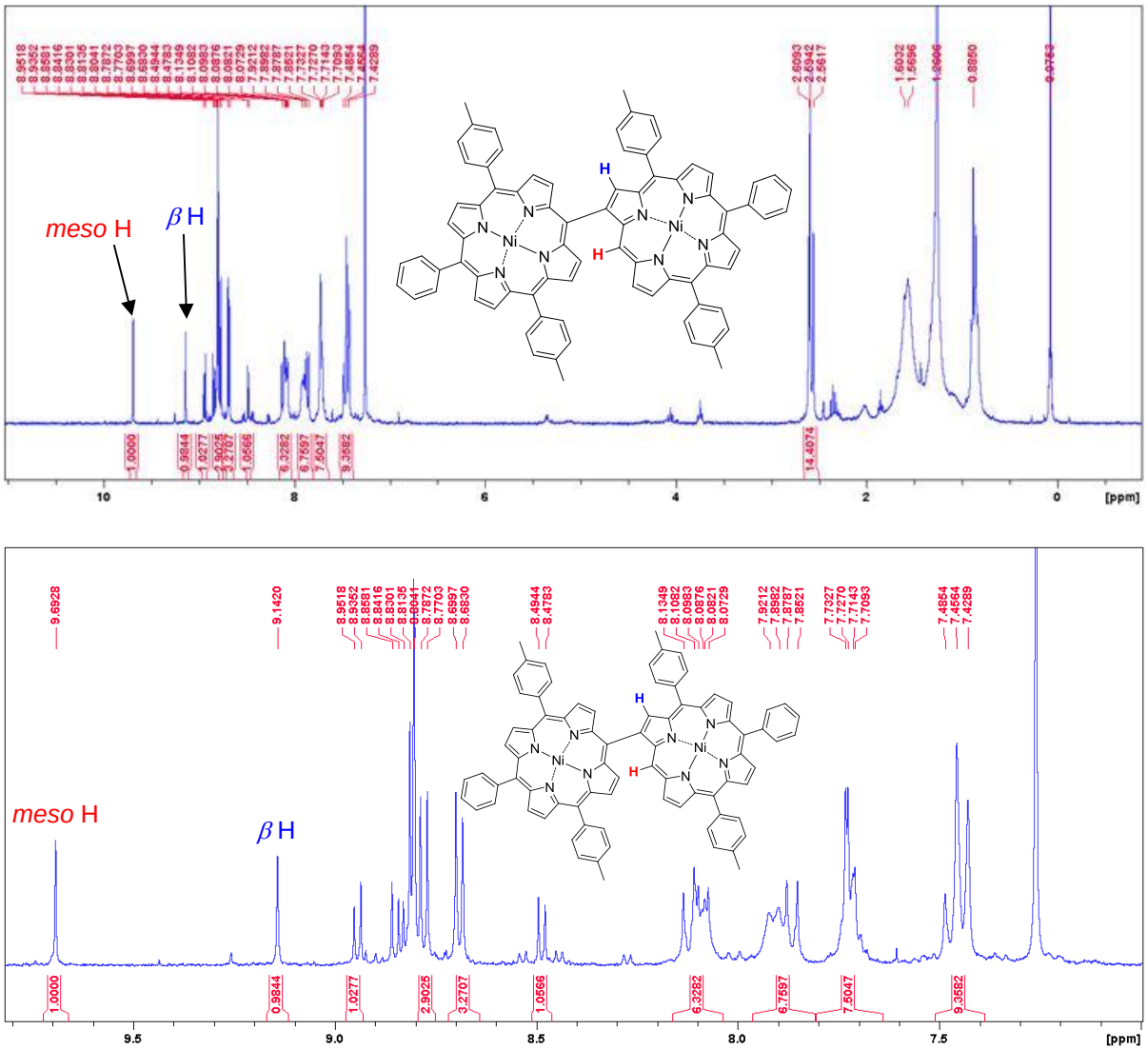

Fig. 43 Full (top) and partial (bottom) ^{1}H NMR spectra of **2'Ni** in $CDCl_3$, 300 MHz, 300 K.

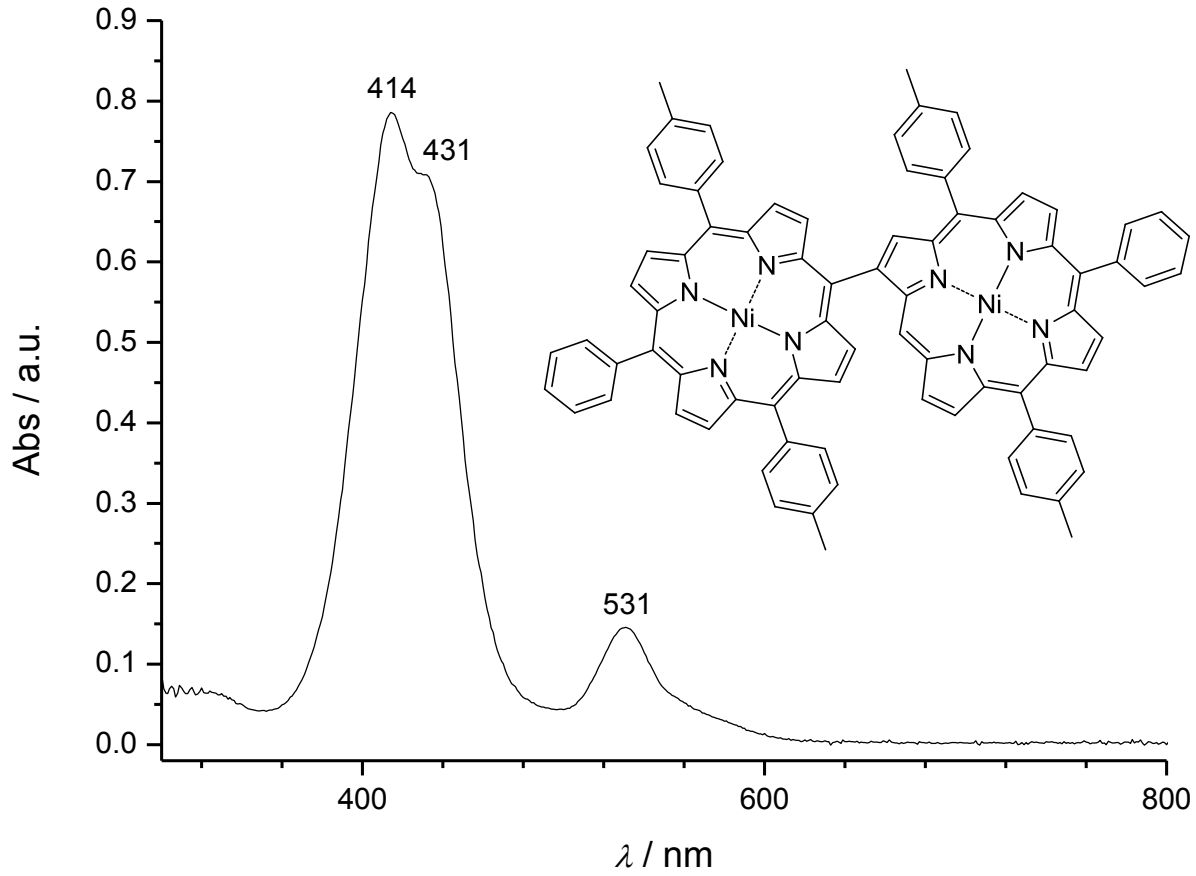

Fig. 44 UV-vis. absorption spectrum of **2'-Ni** in CH_2Cl_2.

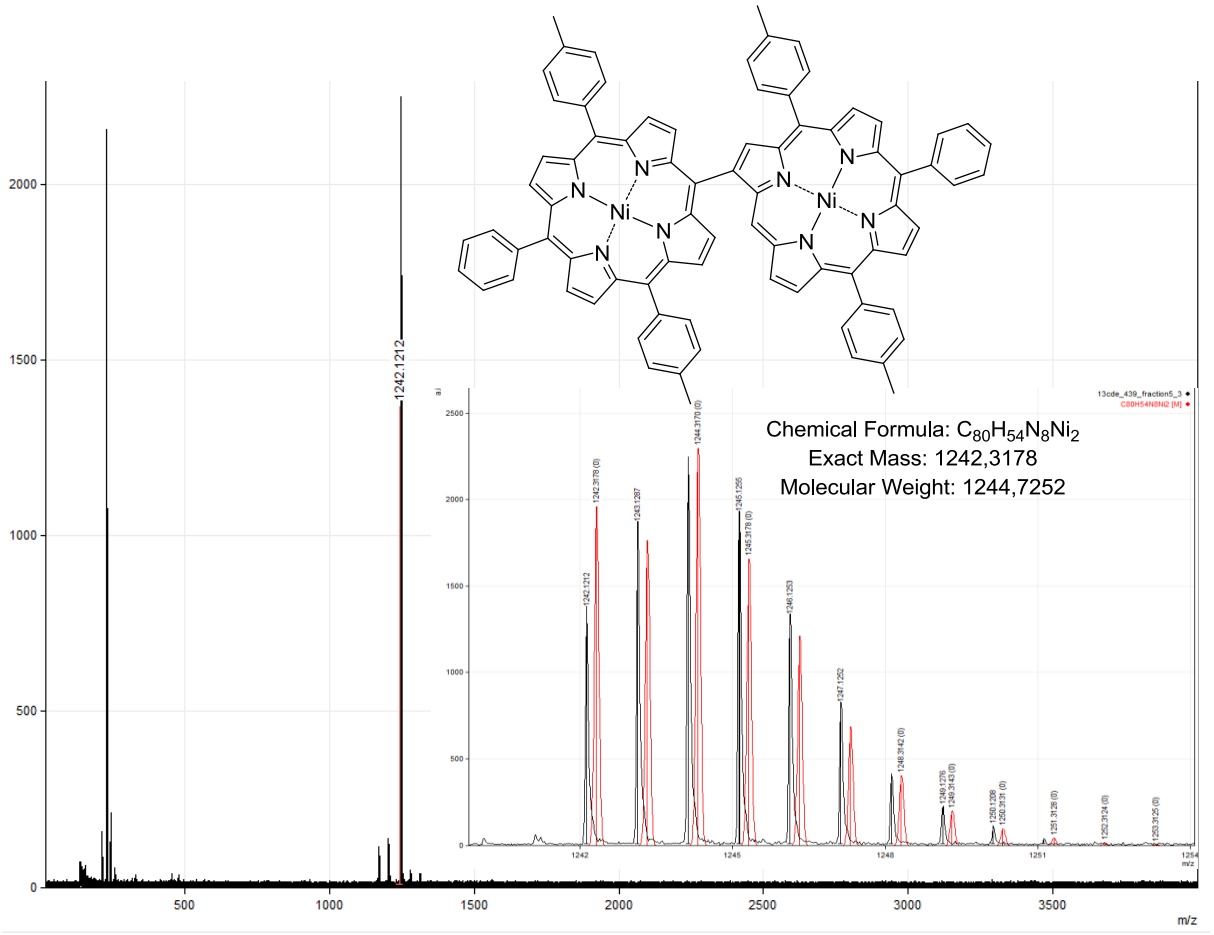

Fig. 45 MALDI-TOF mass spectrum (black) of **2'-Ni**. The magnification shows in red color the simulated isotopic pattern for $C_{80}H_{54}N_8Ni_2$.

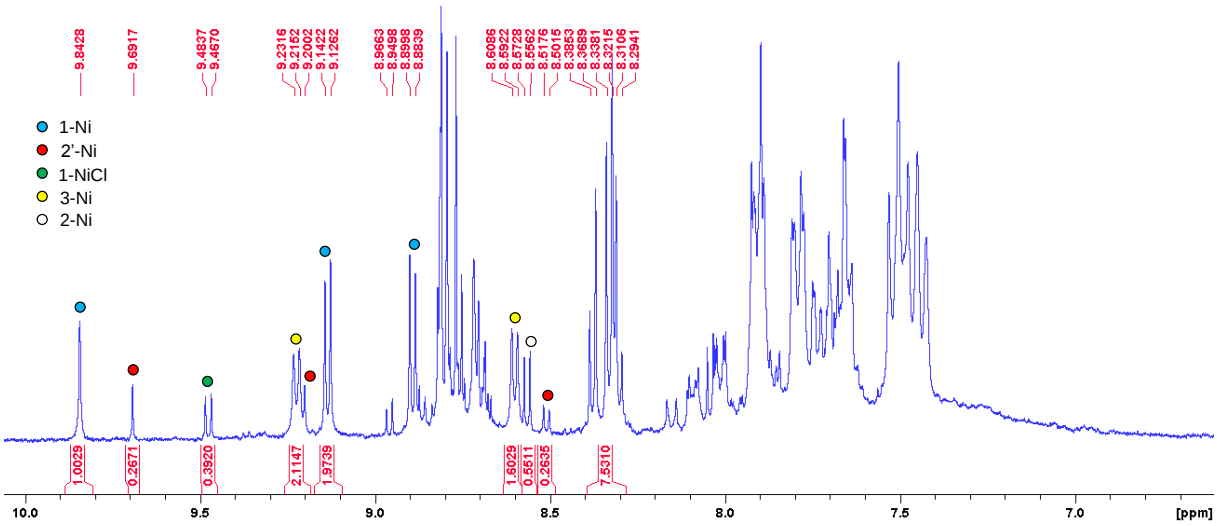

Fig. 46 ^{1}H NMR spectrum obtained for the crude obtained in the conditions of entry 2, Table 1 of the manuscript (CD_2Cl_2, 300 MHz, 300 K).

From this spectrum can be extracted the following data:
Relative amount of monomer units: For **1-Ni** (signal at 9.13 ppm): 1.97/2 H = 0.99 molecule; for **2'-Ni** (signal at 9.69 ppm): 0.27/1 H = 0.27 molecule but as it is a dimer this value has to be multiplied by 2 hence 0.54; for **1-NiCl** (signal at 9.47 ppm): 0.39/2 H = 0.20 molecule; for

3-Ni (signal at 9.22 ppm): (2.11−0.27(integration of **2'-Ni**))/2 H = 0.92 molecule but as it is a dimer this value has to be multiplied by 2 hence 1.84; for **2-Ni** (signal at 8.56 ppm): 0.55/4 H = 0.14 molecule but as it is a dimer this value has to be multiplied by 2 hence 0.28.
Total amount of product: 0.99 + 0.54 + 0.20 + 1.84 + 0.28 = 3.85.
Product's distribution: for **1-Ni**: 0.99/3.85 = 25.7% (~ **26%**); for **2'-Ni**: 0.54/3.85 = **14.0%**; for **1-NiCl**: 0.20/3.85 = 5.2% (~ **5%**); for **3-Ni**: 1.84/3.85 = 47.8% (~ **48%**); for **2-Ni**: 0.28/3.85 = 7.3% (~ **7%**).

Table S1. Crystal and structure refinement data for **1-Ni, 1-Ni-Cl, 1-Ni-P$^+$** and **3-Ni**.

	1 - Ni	**1-Ni-Cl**	**1-Ni-P$^+$**	**3-Ni**
Empirical formula	**$C_{40}H_{28}N_4Ni$**	**$C_{40}H_{27}ClN_4Ni$, C_6H_{14}**	**$C_{58}H_{42}N_4NiP^+$, PF_6^-**	**$C_{80}H_{52}N_8Ni_2$, 0.84(C_5H_{12}), 3.16($CHCl_3$)**
Formula weight	623.37	743.99	1029.61	1680.48
Temperature (K)	115(2)	115(2)	115(2)	115(2)
Crystal system	Orthorhombic	Triclinic	Triclinic	Triclinic
Space group	$P2_12_12_1$	P-1	P-1	P-1
a (Å)	7.8292(4)	11.3951(3)	9.3136(4)	10.1031(7)
b (Å)	17.6253(10)	13.5257(5)	15.5847(6)	14.3045(11)
c (Å)	21.2086(11)	13.7389(5)	16.2590(7)	15.5350(11)
a(°)		109.812(1)	87.634(2)	102.530(2)
β (°)		106.495(2)	83.678(2)	108.384(2)
γ (°)		100.456(2)	84.350(2)	106.350(2)
Volume (Å^3)	2926.6(3)	1817.43(11)	2333.14(17)	1925.7(2)
Z	4	2	2	1
ρ_{calc}. (g/cm^3)	1.415	1.360	1.466	1.449
μ (mm^{-1})	0.701	0.647	0.555	0.871
F(000)	1296	780	1060	852
Crystal size (mm^3)	0.10x0.10x0.02	0.175x0.15x0.15	0.10x0.07x0.05	0.15x0.15x0.10
$\sin(\theta)/\lambda$ max (Å^{-1})	0.65	0.65	0.65	0.65
Index ranges	-10<=h<=10	-14<=h<=14	-12<=h<=12	-13<=h<=13
	-22<=k<=22	-17<=k<=17	-18<=k<=20	-18<=k<=18
	-27<=l<=27	-17<=l<=17	-21<=l<=21	-20<=l<=20
Reflections collected	6511	15454	18462	56882
R_{int}	0.0560	0.0413	0.0747	0.0580
Reflections with $I \geq 2\sigma(I)$	5757	6505	7401	6441
Data / restraints / parameters	6511/0/408	8223 / 0 / 473	10535 / 0 / 643	8851/ 6 / 557
Final *R* indices [$I \geq 2\sigma(I)$]	R1[a] = 0.0783, wR2[b] = 0.1434	R1[a] = 0.0617, wR2[b] = 0.1331	R1[a] = 0.1051, wR2[b] = 0.2069	R1 = 0.0534, wR2 = 0.1237
R indices (all data)	R1[a] = 0.0954, wR2[b] = 0.1532	R1[a] = 0.0844, wR2[b] = 0.1470	R1[a] = 0.1533, wR2[b] = 0.2303	R1 = 0.0809, wR2 = 0.1334
Goodness-of-fit[c] on F^2	1.276	1.129	1.202	1.060
Absolute Structure Parameters	0.08(3)			
Largest difference peak and hole (e Å^{-3})	0.548 -0.502	0.680 -0.528	1.171 -0.554	0.920 -0.612
CCDC deposition no.	981910	981911	981912	981913

[a] $R1=\Sigma(||F_o|-|F_c||)/\Sigma|F_o|$.

[b] $wR2=[\Sigma w(F_o^2-F_c^2)^2/\Sigma[w(F_o^2)^2]^{1/2}$ where $w=1/[\sigma^2(Fo^2+(0.000P)^2+10.6092P]$ for **1-Ni,** $wR2=[\Sigma w(F_o^2-F_c^2)^2/\Sigma[w(F_o^2)^2]^{1/2}$ where $w=1/[\sigma^2(Fo^2+(0.0332P)^2+4.5084P]$ for **1-Ni-Cl,** $w=1/[\sigma^2(Fo^2+21.6158P]$ for **1-Ni-P$^+$,** $w=1/[\sigma^2(Fo^2+(0.0654P)^2+1.1501P]$ for **3-Ni**. where $P=(Max(Fo^2.0)+2*Fc^2)/3$

[c] $S=[\Sigma w(F_o^2-F_c^2)^2/(n-p)]^{1/2}$ (*n* = number of reflections. *p* = number of parameters).

1. A. Tsuda, Y. Nakamura and A. Osuka, *Chem. Commun.*, 2003, 1096.